Molecular Meccano. 2. Self-Assembly of [n]Catenanes[1]

David B. Amabilino,[†] Peter R. Ashton,[†] Christopher L. Brown,[†] Emilio Córdova,[‡] Luis A. Godínez,[‡] Timothy T. Goodnow,[‡] Angel E. Kaifer,[‡] Simon P. Newton,[†] Marek Pietraszkiewicz,[†] Douglas Philp,[†] Françisco M. Raymo,[†] Anatoli S. Reder,[†] Marcus T. Rutland,[†] Alexandra M. Z. Slawin,[⊥] Neil Spencer,[†] J. Fraser Stoddart,*[,†] and David J. Williams*[,⊥]

Contribution from The School of Chemistry, The University of Birmingham, Edgbaston, Birmingham B15 2TT, U.K., Department of Chemistry, University of Miami, Coral Gables, Florida 33124, and Department of Chemistry, Imperial College, London SW7 2AY, U.K.

Received August 25, 1994[⊗]

Abstract: The mutual molecular recognition between different structural components in large rings has led to the template-directed synthesis of a wide range of catenanes composed of from two to five interlocked rings. The molecular self-assembly processes rely upon the recognition between (i) π-electron rich and π-electron deficient aromatic units and (ii) hydrogen bond donors and acceptors, in the different components. In order to increase our knowledge of the factors involved in such molecular self-assembly processes, a homologous series of [2]catenanes has been constructed using macrocyclic polyethers of the bis(*p*-phenylene)-(3*n*+4)-crown-*n* (n = 9−14) type as templates for the formation of the tetracationic cyclophane, cyclobis(paraquat-*p*-phenylene). Increasing the size of the tetracationic cyclophane to cyclobis(paraquat-4,4′-bitolyl) allows the simultaneous entrapment of two hydroquinone ring-containing macrocyclic polyethers affording a series of [3]catenanes, and one [4]catenane incorporating a cyclic dimer of the expanded cyclophane and three bis(*p*-phenylene)-34-crown-10 components. By analogy, increasing the number of hydroquinone rings in the macrocyclic polyether permits the self-assembly of more than one tetracationic cyclophane around the templates present in the macrocyclic polyether. In this context, the template-directed synthesis of two [3]catenanes, incorporating two cyclobis(paraquat-*p*-phenylene) components and either (i) tris(*p*-phenylene)-51-crown-15 or (ii) tetrakis(*p*-phenylene)-68-crown-20, has been achieved and is reported. A combination of these two approaches has led to the successful self-assembly, in two steps, of a linear [4]catenane, together with a small amount of a [5]catenane. The creation of these intricate molecular compounds lends support to the contention that self-assembly is a viable paradigm for the construction of nanometer-scale molecular architectures incorporating a selection of simple components.

Self-assembly[2] is an extremely powerful tool for the creation of extremely large, highly ordered, and functioning molecular and supramolecular systems. Chemists[3] are now uncovering totally synthetic self-assembling, self-organizing, and self-replicating systems which mimic, in a modest manner, their natural role models. In order to make the transition from the creation of these relatively small and simple unnatural molecular and supramolecular structures to well-defined nanometer-scale superstructures, it is necessary to understand and then optimize the molecular recognition between the precursor components of the synthetic system. The accumulation of this knowledge could lead[4] ultimately to the rapid generation of totally synthetic, highly organized, and functioning molecular and supramolecular systems.[5−8]

Molecular compounds incorporating an aspect of mechanical interlocking[9] constitute another appealing structural motif to target using self-assembly. The catenanes, rotaxanes, and knots[10] were originally curiosities, prepared in very low yields, by statistical synthetic methods. The advent of the template-directed approach, developed in the first instance largely by Sauvage and co-workers,[11] helped to turn these curios into accessible structures. Thus, catenanes, rotaxanes, and knots are ideal target structures to be made to order by self-assembly processes. The beauty of the interlocking is that the molecular recognition, which facilitates the creation of their molecular structures, remains alive inside the molecules once they have been formed.[12]

† The University of Birmingham.
‡ University of Miami.
⊥ Imperial College.
⊗ Abstract published in *Advance ACS Abstracts,* December 15, 1994.

(1) Anelli, P. L.; Ashton, P. R.; Ballardini, R.; Balzani, V.; Delgado, M.; Gandolfi, M. T.; Goodnow, T. T.; Kaifer, A. E.; Philp, D.; Pietraszkiewicz, M.; Prodi, L.; Reddington, M. V.; Slawin, A. M. Z.; Spencer, N.; Stoddart, J. F.; Vicent, C.; Williams, D. J. *J. Am. Chem. Soc.* **1992**, *114*, 193−218.

(2) (a) Lindsey, J. S. *New J. Chem.* **1991**, *15*, 153−180. (b) Whitesides, G. M.; Mathias, J. P.; Seto, C. T. *Science* **1991**, *254*, 1312−1319.

(3) For recent examples of synthetic self-assembling systems, see: (a) Menger, F. M.; Littau, C. A. *J. Am. Chem. Soc.* **1993**, *115*, 10083−10090. (b) Kotera, M.; Lehn, J.-M.; Vigneron, J.-P. *J. Chem. Soc., Chem. Commun.* **1994**, 197−198. (c) Mathias, J. P.; Simanek, E. E.; Whitesides, G. M. *J. Am. Chem. Soc.* **1994**, *116*, 4326−4340. (d) Wyler, R.; de Mendoza, J.; Rebek, Jr., *J. Angew. Chem., Int. Ed. Engl.* **1993**, *32*, 1699−1701. (e) Copp, S. B.; Subramanian, S.; Zaworotko, M. J. *Angew. Chem., Int. Ed. Engl.* **1993**, *32*, 706−709. (f) Thonden van Velzen, E. U.; Engbersen, J. F. J.; Reinhoudt, D. N. *J. Am. Chem. Soc.* **1994**, *116*, 3597−3598. (g) Ziessel, R.; Youinou, M.-T. *Angew. Chem., Int. Ed. Engl.* **1993**, *32*, 877−880. (h) Yang, J.; Fan, E.; Geib, S. J.; Hamilton, A. D. *J. Am. Chem. Soc.* **1993**, *115*, 5314−5315. Self-organizing systems have been described: (i) Serrette, A. G.; Swager, T. M. *J. Am. Chem. Soc.* **1993**, *115*, 8879−8880. (j) Fujita, K.; Kimura, S.; Imanishi, Y.; Rump, E.; Ringsdorf, H. *J. Am. Chem. Soc.* **1994**, *116*, 2185−2186. (k) Joachimi, D.; Tschierske, C.; Müller, H.; Wendorff, J. H.; Schneider, L.; Kleppinger, R. *Angew. Chem., Int. Ed. Engl.* **1993**, *32*, 1165−1167. (l) Krafft, M.-P.; Giulieri, F.; Reiss, J. G. *Angew. Chem., Int. Ed. Engl.* **1993**, *32*, 741−743. Artificial self-replicating molecules have been reported: (m) Achilles, T.; von Kiedrowski, G. *Angew. Chem., Int. Ed. Engl.* **1993**, *32*, 1198−1201. (n) Feng, Q.; Park, T. K.; Rebek Jr., J. *Science* **1992**, *256*, 1179−1180. (o) Menger, F. M.; Eliseev, A. V.; Khanjin, N. A. *J. Am. Chem. Soc.* **1994**, *116*, 3613−3614. (p) Bachmann, P. A.; Luisi, P. L.; Lang, J. *Nature* **1992**, *357*, 57−59. (q) Hoffmann, S. *Angew. Chem., Int. Ed. Engl.* **1992**, *31*, 1013−1016. (r) Li, T.; Nicolau, K. C. *Nature* **1994**, *369*, 218−221. (s) Sievers, D.; von Kiedrowski, G. *Nature* **1994**, *369*, 221−224.

(4) Lehn, J.-M. *Science* **1993**, *260*, 1762−1763.

0002-7863/95/1517-1271$09.00/0

The complexation of π-electron deficient units—*e.g.*, the paraquat dication[13]—by macrocyclic ethers containing π-electron rich aromatic rings—*e.g.*, hydroquinone rings[14]—has provided[15] the inspiration for the self-assembly[16] of a number of interlocked and intertwined structures based on these and related building blocks. In the first paper in this series, we reported the template-directed[17] synthesis of a range of [2]rotaxanes and one [2]-catenane.[1] It provided some initial insight relating to the key structural features that are necessary for self-assembly to operate in these molecular systems. Further insight is required in order that the efficiencies of the catenane-forming reactions can be tuned so that nanometer-scale architectures can be self-assembled with ease. Linear polycatenanes[18] are appealing and synthetically challenging unnatural products. Self-assembly provides one of the most highly controlled and efficient methods for the construction of these molecular chains. Here, we describe the recent progress that has been made toward a deeper understanding of the self-assembly processes by which a range of catenanes have been produced. They rely upon incorporating 4,4′-bipyridinium units and hydroquinone rings into the template-directed synthesis of a homologous series of [2]catenanes and [3]catenanes, as forerunners to some larger catenane arrays, including linear [4]- and [5]catenanes. X-ray crystallography, mass spectrometry, NMR spectroscopy, and electrochemistry have all been used to establish the molecular structures of these novel compounds.

Results and Discussion

Names and Cartoons. It will be convenient in presenting the results to employ acronyms composed of letters, and occasionally numbers, to identify the neutral and charged compounds displayed in the figures and schemes. Thus, bis-(*p*-phenylene)-(3*n*+4)-crown-*n* is abbreviated to BPP(3*n*+4)-C*n*, where *n* represents the number of oxygen atoms in the macrocycle. Tris(*p*-phenylene)-51-crown-15 is abbreviated to TPP51C15, and tetrakis(*p*-phenylene)-68-crown-20 to TPP68C20. The other acronyms employed in the figures and schemes can be deduced on the basis of the following definitions: B stands for bis when at the beginning, for benzyloxy or bromomethyl when in the middle, and for benzene when at the end of the name. B stands for benzyloxy when it is present in the acronyms of neutral compounds, and for bromomethyl when it is present in those of charged compounds. E, H, P, and T stand for ethoxy, hydroxy, phenoxy, and tosyloxy, respectively. BT, CY, DO, PH, TT, TU, XY, BIBT, and BIXY represent bitolyl, cyclophane, dioxaoctane, pentaoxaheptadecane, tetraoxatetradecane, trioxaundecane, xylylene, bisbitolyl, and bisxylylene units, respectively. In addition, BP and BIPY stand for bipyridine and the bipyridinium ring system, respectively. The formal charges are indicated in the usual manner. In the cartoon

(5) Double helices assembled using metal ion coordination have been reviewed: Constable, E. C. *Tetrahedron* **1992**, *48*, 10013–10059. For more recent examples, see: (a) Carina, R. F.; Bernardinelli, G.; Williams, A. F. *Angew. Chem., Int. Ed. Engl.* **1993**, *32*, 1463–1465. (b) Constable, E. C.; Edwards, A. J.; Raithby, P. R.; Walker, J. V. *Angew. Chem., Int. Ed. Engl.* **1993**, *32*, 1465–1467. (c) Krämer, R.; Lehn, J.-M.; Marquis-Rigault, A. *Proc. Natl. Acad. Sci. U.S.A.* **1993**, *90*, 5394–5398. A solid state hydrogen-bonded double helix has been described: Geib, S. J.; Vicent, C.; Fan, E.; Hamilton, A. D. *Angew. Chem., Int. Ed. Engl.* **1993**, *32*, 119–121.

(6) Watson, J. D.; Crick, F. H. C. *Nature* **1953**, *171*, 737–738.

(7) For reports on triple helices self-assembled using metal ion templates, see: (a) Bernardinelli, G.; Piguet, C.; Williams, A. F. *Angew. Chem., Int. Ed. Engl.* **1992**, *31*, 1622–1624. (b) Krämer, R.; Lehn, J.-M.; De Cian, A.; Fischer, J. *Angew. Chem., Int. Ed. Engl.* **1993**, *32*, 703–706. A solid state hydrogen-bonded triple-stranded helicate has been described: Hanessian, S.; Gomtsyan, A.; Simard, M.; Roelens, S. *J. Am. Chem. Soc.* **1994**, *116*, 4495–4496.

(8) Percec, V.; Heck, J.; Lee, M.; Ungar, G.; Alvarez-Castillo, A. *J. Mater. Chem.* **1993**, *2*, 1033–1039.

(9) Mechanical interlocking requires the presence of "topological" bonds between components comprised of covalently bonded atoms; see: (a) Frisch, H. L.; Wasserman, E. *J. Am. Chem. Soc.* **1961**, *83*, 3789–3795. (b) Walba, D. M. *Tetrahedron* **1985**, *41*, 3191–3212. (c) Chambron, J.-C.; Dietrich-Buchecker, C. O.; Sauvage, J.-P. *Top. Curr. Chem.* **1993**, *165*, 131–162. (d) van Gulick, N. *New J. Chem.* **1993**, *17*, 619–625. (e) Weber, C. *New J. Chem.* **1993**, *17*, 627–644. (f) Schücker, T. *New J. Chem.* **1993**, *17*, 655–660. (g) Frisch, H. L. *New J. Chem.* **1993**, *17*, 697–701.

(10) (a) Schill, G. *Catenanes, Rotaxanes and Knots*; Academic Press: New York, 1971. (b) Dietrich-Buchecker, C. O.; Sauvage, J.-P. In *Bioorganic Chemistry Frontiers*; Dugas, H., Ed.; Springer-Verlag: Berlin, 1991; Vol. 2, pp 195–248. For more recent reports on catenanes, see: (c) Hunter, C. A. *J. Am. Chem. Soc.* **1992**, *114*, 5303–5311. (d) Vögtle, F.; Meier, S.; Hoss, R. *Angew. Chem., Int. Ed. Engl.* **1992**, *31*, 1619–1621. (e) Carver, F. J.; Hunter, C. A.; Shannon, R. J. *J. Chem. Soc., Chem. Commun.* **1994**, 1277–1280. (f) Gruter, G.-J. M.; de Kanter, F. J. J.; Markies, P. R.; Nomoto, T.; Akkerman, O. S.; Bickelhaupt, F. *J. Am. Chem. Soc.* **1993**, *115*, 12179–12180. (g) Armspach, D.; Ashton, P. R.; Moore, C. P.; Spencer, N.; Stoddart, J. F.; Wear, T. J.; Williams, D. J. *Angew. Chem., Int. Ed. Engl.* **1993**, *32*, 854–858. (h) Fujita, M.; Ibukuro, F.; Hagihara, H.; Ogura, K. *Nature* **1994**, *367*, 720–723. Rotaxanes have recently been reported: (i) Markies, P. R.; Nomoto, T.; Akkerman, O. S.; Bickelhaupt, F. *J. Am. Chem. Soc.* **1988**, *110*, 4845–4846. (j) Chambron, J.-C.; Heitz, V.; Sauvage, J.-P. *J. Am. Chem. Soc.* **1993**, *115*, 12378–12384. (k) Wenz, G.; von der Bey, E.; Schmidt, L. *Angew. Chem., Int. Ed. Engl.* **1992**, *31*, 783–785. (l) Wenz, G.; Wolf, F.; Wagner, M.; Kubik, S. *New J. Chem.* **1993**, *17*, 729–738. (m) Isnin, R.; Kaifer, A. E. *J. Am. Chem. Soc.* **1991**, *113*, 8188–8190. For a report on molecular knots, see: (n) Dietrich-Buchecker, C. O.; Nierengarten, J.-F.; Sauvage, J.-P.; Armaroli, N.; Balzani, V.; De Cola, L. *J. Am. Chem. Soc.* **1993**, *115*, 11237–11244. For recent reports concerning the construction of interlocked structures comprised of DNA, see: (o) Seeman, N. C.; Chen, J.; Du, S. M.; Mueller, J. E.; Zhang, Y.; Fu, T.-J.; Wang, Y.; Wang, H.; Zhang, S. *New J. Chem.* **1993**, *17*, 739–755. (p) Shekhtman, E. M.; Wasserman, S. A.; Cozzarelli, N. R.; Solomon, M. J. *New J. Chem.* **1993**, *17*, 757–763. (q) Stark, W. M.; Parker, C. N.; Halford, S. E.; Boocock, M. R. *Nature* **1994**, *368*, 76–78. (r) Zhang, Y.; Seeman, N. C. *J. Am. Chem. Soc.* **1994**, *116*, 1661–1669.

(11) For a review on the metal ion templated formation of catenantes, see: Sauvage, J.-P. *Bull. Soc. Chim. Fr.* **1992**, *128*, 113–120. For the recent synthesis of a doubly interlocked [2]catenane, see: Nierengarten, J.-F.; Dietrich-Buchecker, C. O.; Sauvage, J.-P. *J. Am. Chem. Soc.* **1994**, *116*, 375–376.

(12) The intermolecular noncovalent bonds responsible for the self-assembly of the catenanes of the type described here remain evident in the solution and solid state structures of the interlocked rings. See: Ashton, P. R.; Goodnow, T. T.; Kaifer, A. E.; Reddington, M. V.; Slawin, A. M. Z.; Spencer, N.; Stoddart, J. F.; Vicent, C.; Williams, D. J. *Angew. Chem., Int. Ed. Engl.* **1989**, *28*, 1396–1399.

(13) For examples of paraquat receptors, see: (a) Ashton, P. R.; Chrystal, E. J. T.; Mathias, J. P.; Parry, K. P.; Slawin, A. M. Z.; Spencer, N.; Stoddart, J. F.; Williams, D. J. *Tetrahedron Lett.* **1987**, *28*, 6367–6370. (b) Bernardo, A. R.; Lu, T.; Córdova, E.; Zhang, L.; Gokel, G. W.; Kaifer, A. E. *J. Chem. Soc., Chem. Commun.* **1994**, 529–530. (c) Gunter, M. J.; Johnston, M. R.; Skelton, B. W.; White, A. H. *J. Chem. Soc., Perkin Trans. 1* **1994**, 1009–1018.

(14) Stoddart, J. F. *Pure Appl. Chem.* **1988**, *60*, 467–472.

(15) Amabilino, D. B.; Stoddart, J. F.; Williams, D. J. *Chem. Mater.* **1994**, *6*, 1159–1167.

(16) (a) Philp, D.; Stoddart, J. F. *Synlett* **1991**, 445–458. For reports on rotaxanes based on these systems, see: (b) Sun, X.; Amabilino, D. B.; Ashton, P. R.; Parsons, I. W.; Stoddart, J. F.; Tolley, M. S. *Macromol. Symp.* **1994**, *77*, 191–207. (c) Benniston, A. C.; Harriman, A.; Lynch, V. M. *Tetrahedron Lett.* **1994**, *35*, 1473–1476. (d) Córdova, E.; Bissell, R. A.; Spencer, N.; Ashton, P. R.; Stoddart, J. F.; Kaifer, A. E. *J. Org. Chem.* **1993**, *58*, 6550–6552. For reports on catenanes based on this system, see: (e) Amablino, D. B.; Stoddart, J. F. *Recl. Trav. Chim. Pays-Bas* **1993**, *112*, 429–430. (f) Vögtle, F.; Müller, W. M.; Müller, U.; Bauer, M.; Rissanen, K. *Angew. Chem., Int. Ed. Engl.* **1993**, *32*, 1295–1297. (g) Gunter, M. J.; Hockless, D. C. R.; Johnston, M. R.; Skelton, B. W.; White, A. H. *J. Am. Chem. Soc.* **1994**, *116*, 4810–4823.

(17) For reviews on the use of templates in organic synthesis, see: (a) Busch, D. H. *J. Inclusion Phenom.* **1992**, *12*, 389–395. (b) Anderson, S.; Anderson, H. L.; Sanders, J. K. M. *Acc. Chem. Res.* **1993**, *26*, 469–475. (c) Hoss, R.; Vögtle, F. *Angew. Chem., Int. Ed. Engl.* **1994**, *33*, 375–384.

(18) A single macrocyclization reaction has afforded nonlinear [3]-, [4]-, [5]-, [6]- and [7]catenates. See: (a) Dietrich-Buchecker, C. O.; Guilhem, J.; Khémiss, A.-K.; Kintzinger, J.-P.; Pascard, C.; Sauvage, J.-P. *Angew. Chem., Int. Ed. Engl.* **1987**, *26*, 661–663. (b) Bitsch, F.; Dietrich-Buchecker, C. O.; Khémiss, A.-K.; Sauvage, J.-P.; Dorsselaer, A. V. *J. Am. Chem. Soc.* **1991**, *113*, 4023–4025. More recently, three rings have been templated around a macrobicyclic "core". See: Dietrich-Buchecker, C. O.; Frommberger, B.; Lüer, I.; Sauvage, J.-P.; Vögtle, F. *Angew. Chem., Int. Ed. Engl.* **1993**, *32*, 1434–1437.

Scheme 1

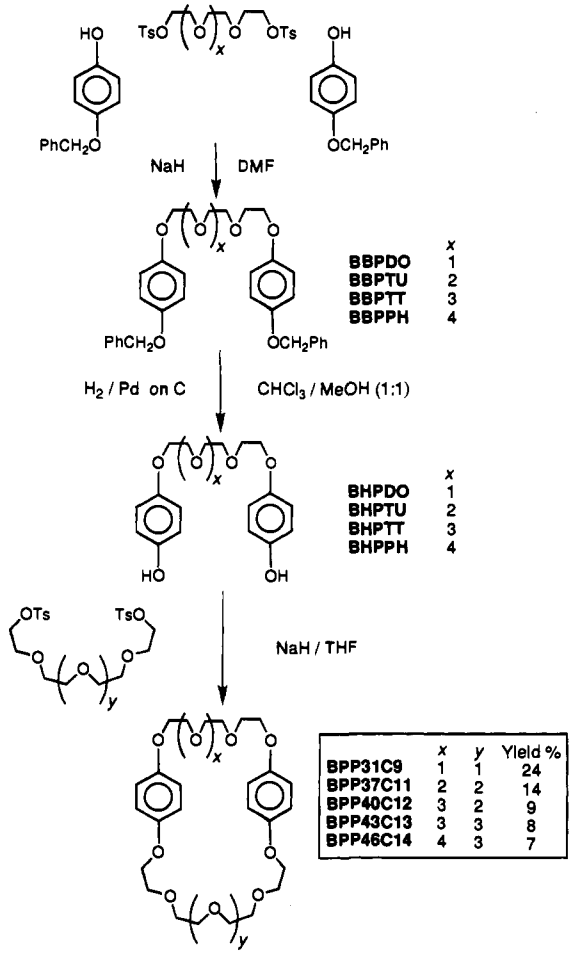

versions of the structural formulas displayed in the figures and schemes, smaller rectangles represent *para*-disubstituted benzene rings, whereas the larger ones represent bipyridinium ring systems. In neutral molecules, the rectangles are unshaded, whereas they are shaded black in the case of the positively-charged organic species, with the formal charges positioned appropriately.

Synthesis. The homologous series of bis(*p*-phenylene) macrocyclic polyethers BPP(3*n*+4)C*n* (where $n = 9$ and 11–14) was prepared (Scheme 1) from the appropriate oligoethylene glycol bistosylates.[19] Better yields were obtained when the same reactions were carried out in DMF using cesium carbonate as the base in the presence of cesium tosylate.[20]

The [2]catenane {[2]-[BPP34C10]-[BBIPYBIXYCY]catenane}-$[PF_6]_4$ has been prepared[1] in 70% yield from $[BBIPYXY][PF_6]_2$, 1,4-bis(bromomethyl)benzene (BBB), and the crown ether. The catenane can also be prepared[21] in 18% yield starting from 4,4′-bipyridine (BP), BBB, and BPP34C10 at room temperature and pressure (Scheme 2). Upon resorting to high pressure, the catenane was isolated in 42% yield, a result which demonstrates the utility of these conditions for the self-assembly of this type of catenane. Reaction of an excess of BBB with BP yielded the intermediate dicationic dibromide $[BBXYBIPY]^{2+}$, which

(19) Ouchi, M.; Inoue, Y.; Liu, Y.; Nagamune, S.; Nakamura, S.; Wada, K.; Hakushi, K. *Bull. Chem. Soc. Jpn.* **1990**, *63*, 1260–1262.

(20) For a review on the "cesium effect" in the synthesis of macrocyclic compounds, see: (a) Ostrowicki, A.; Koepp, E.; Vögtle, F. *Top. Curr. Chem.* **1991**, *161*, 37–67. See also: (b) Dijkstra, G.; Kruizinga, W. H.; Kellogg, R. M. *J. Org. Chem.* **1987**, *52*, 4230–4234. (c) Galli, C.; Mandolini, L. *J. Org. Chem.* **1991**, *56*, 3045–3047.

(21) Brown, C. L.; Philp, D.; Stoddart, J. F. *Synlett* **1991**, 459–461.

Scheme 2

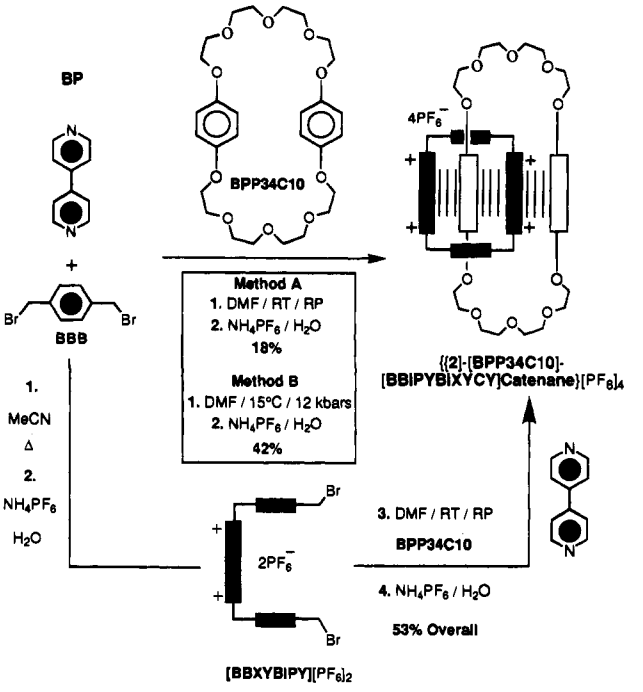

Scheme 3

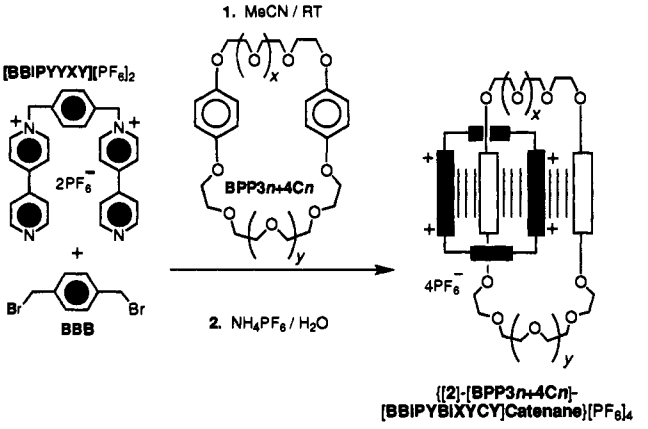

	x	y	Yield %
{[2]-[BPP31C9]-[BBIPYBIXYCY]Catenane}$[PF_6]_4$	1	1	10
{[2]-[BPP34C10]-[BBIPYBIXYCY]Catenane}$[PF_6]_4$	2	1	70
{[2]-[BPP37C11]-[BBIPYBIXYCY]Catenane}$[PF_6]_4$	2	2	55
{[2]-[BPP40C12]-[BBIPYBIXYCY]Catenane}$[PF_6]_4$	3	2	54
{[2]-[BPP43C13]-[BBIPYBIXYCY]Catenane}$[PF_6]_4$	3	3	40
{[2]-[BPP46C14]-[BBIPYBIXYCY]Catenane}$[PF_6]_4$	4	3	49

was used without further purification for the self-assembly of {[2]-[BPP34C10]-[BBIPYBIXYCY]catenane}$[PF_6]_4$ in 53% yield.

The efficiency of the clipping procedure led to its use for the preparation of the {[2]-[BPP(3*n*+4)C*n*]-[BBIPYBIXYCY]-catenane}s with $n = 9$ and 11–14 as their tetrakis(hexafluorophosphate) salts (Scheme 3), starting from an excess of the appropriate bis(*p*-phenylene) crown ether, $[BBIPYXY][PF_6]_2$, and 1,4-bis(bromomethyl)benzene (BBB). The maximum yield from the clipping procedure is realized[1] when BPP34C10 is employed. Although, when the smaller BPP31C9 is used, the clipping procedure is rather inefficient, when crown ethers larger than BPP34C10 are employed, only a modest attenuation in the efficiency of the self-assembly process is observed. This result is at variance with the behavior expected if the clipping efficiency was directly related to the ability (Figure 1) of the

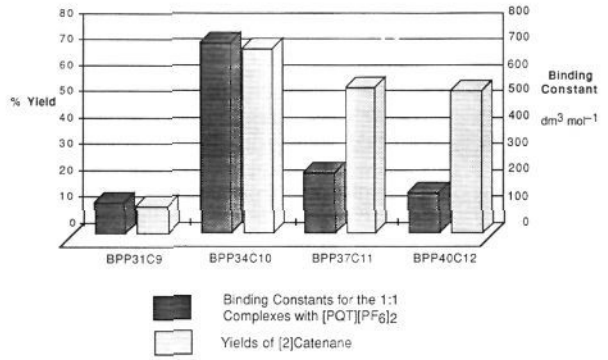

Figure 1. A bar-chart comparison of the binding constants of the crown ethers BPP(3*n*+4)C*n* (*n* = 9−14) with $[PQT][PF_6]_2$ in Me_2CO and the yields obtained in the self-assembly of the {[2]-[BPP(3*n*+4)C*n*]-[BBIPYBIXYCY]catenane}s in acetonitrile at room temperature and pressure.

crown ether to bind paraquat.[22] The $[BBIPYXY]^{2+}$ ion is not bound appreciably by the macrocyclic polyethers, while the intermediate trication $[BBIPYXYBXY]^{3+}$ incorporates one paraquat-like residue and is presumably therefore bound by the macrocyclic polyethers. If there is a strong dependence of clipping efficiencies on binding constants, we should observe inefficient clipping with both small *and* large crown sizes. The macrocyclic template BPP31C9 might be expected to exhibit a low efficiency during its catenation when compared with the corresponding catenation of BPP34C10. In the case of BPP31C9, it is difficult to fit a paraquat residue inside its cavity. The larger macrocyclic receptors bind the $[PQT]^{2+}$ dication less well than does BPP34C10. Presumably, this trend is a result of their poorer preorganization, which is apparently not as pernicious as it might have been to the efficiency of catenation with the $[BBIPYBIXYCY]^{4+}$ cyclophane. This observation is not surprising, since an acyclic threadlike molecule containing one hydroquinone residue is capable of templating the formation of the cyclophane in 35% yield.[1]

In an attempt to gain an understanding of the reasons behind this difference, we decided to investigate[23] the formation of the {[2]-[BPP34C10]-[BBIPYBIXYCY] catenane}$[PF_6]_4$. We need to consider (Figure 2) two possible limiting kinetic scenarios which could prevail during the reaction which creates this [2]-catenane. In both situations, the rate constant for complexation is assumed to be much larger than those (k_1 and k_2) associated with the two covalent bond-forming steps. Scenario I assumes that the first step, *i.e.*, the alkylation of $[BBIPYXY]^{2+}$, is the rate-limiting step; *i.e.*, k_1 is small with respect to k_2. We can predict that, if scenario I is correct, then monitoring the contents of the reaction mixture should only reveal the disappearance of $[BBIPYXY]^{2+}$ and BBB, and the appearance of the [2]catenane. In scenario II, k_2 is less than k_1; *i.e.*, the second ring-closing alkylation is rate-determining. Thus, if scenario II is correct, then monitoring the contents of the reaction mixture should reveal a system which changes rapidly with time from one involving the reactants to an intermediate state, and then slowly on to the products. This scenario should permit the observation spectroscopically of the intermediate tricationic complex $[BPP34C10{\cdot}BBIPYXYBXY]^{3+}$. We reasoned that it should be possible to follow the formation of the [2]catenane by ^1H NMR spectroscopy; consequently, the ingredients $[BBIPYXY][PF_6]_2$, BPP34C10, and BBB were all dissolved in dimethylformamide-

(22) Ashton, P. R.; Slawin, A. M. Z.; Spencer, N.; Stoddart, J. F.; Williams, D. J. *J. Chem. Soc., Chem. Commun.* **1987**, 1066−1069.
(23) Brown, C. L.; Philp, D.; Spencer, N.; Stoddart, J. F. *Isr. J. Chem.* **1992**, *32*, 61−67.

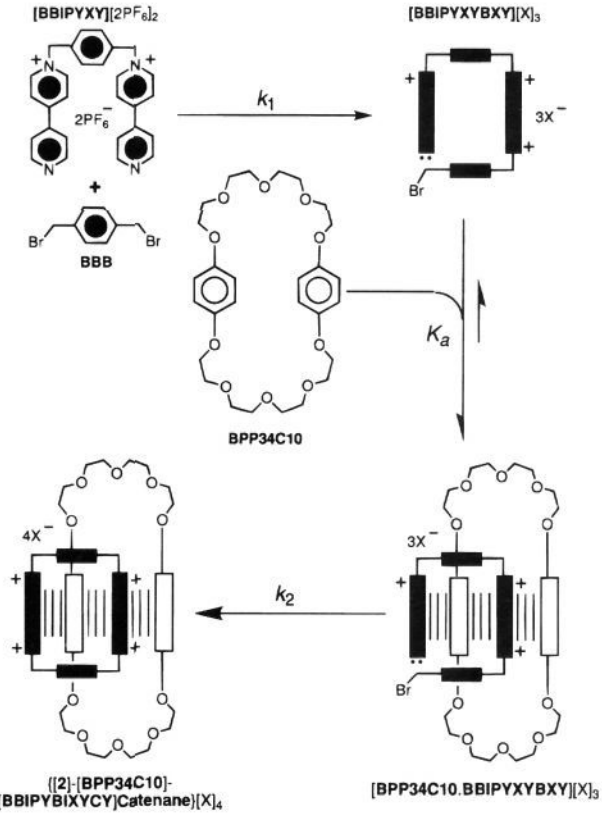

Figure 2. A proposed mechanism for the formation of {[2]-[BPP34C10]-[BBIPYBIXYCY]catenane}$^{4+}$.

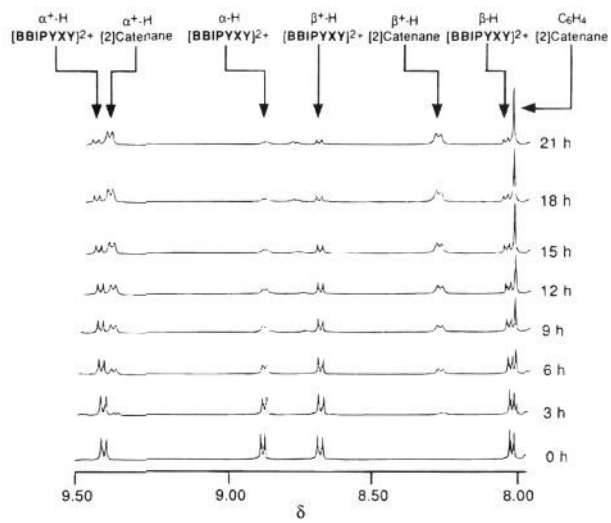

Figure 3. Low field region of the ^1H NMR spectrum in DMF-d_7 (with a drop of D_2O) showing the formation of {[2]-[BPP34C10]-[BBIPY-BIXYCY]catenane}$^{4+}$ with time.

d_7 and placed in an NMR tube. One drop of D_2O was then added to the resulting colorless solution to prevent precipitation of the products of the reaction.

The changes in the 400 MHz ^1H NMR spectra of this mixture were followed during the subsequent 60 h, one spectrum being recorded automatically every hour. Figure 3 shows the region of the spectrum between δ 8.00 and δ 9.50. The resonances for the quaternized and unquarternized bipyridine protons fall in this range. At the start of the experiment, only four resonances were evident, corresponding to the four different types of pyridylpyridinium protons in the $[BBIPYXY]^{2+}$ dication. After 3 h, the intensity of the four original resonances

Scheme 4

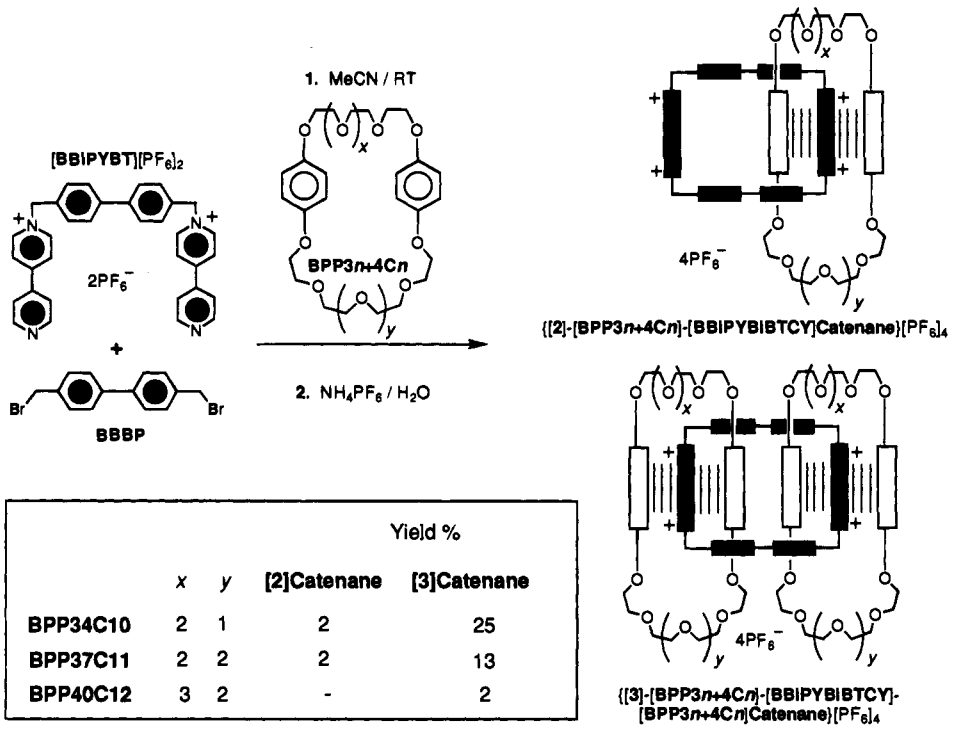

			Yield %	
	x	*y*	[2]Catenane	[3]Catenane
BPP34C10	2	1	2	25
BPP37C11	2	2	2	13
BPP40C12	3	2	-	2

was noticeably diminished and three additional resonances started to appear. The three new resonances correspond to the protons in the tetracationic [BBIPYBIXYCY]$^{4+}$ component of the [2]catenane. They are, from low to high field, the α-CH protons of the [BIPY]$^{2+}$ unit, the β-CH protons of the [BIPY]$^{2+}$ unit, and the aromatic protons of the bridging C_6H_4 unit. Over the remaining period of the experiment, the three new resonances continued to grow in intensity while the original four resonances diminished in intensity. In this region of the ^{1}H NMR spectrum, if any other species were present in solution, they must have existed at extremely low concentrations. This observation was supported by examination in the region of the ^{1}H NMR spectrum between δ 6.00 and δ 6.30. The resonances, corresponding to the methylene groups adjacent to the quaternary nitrogen centers in both the [BBIPYXY]$^{2+}$ dication and the [BBIPYBIXYCY]$^{4+}$ component of the [2]catenane, appear in this region. It might reasonably be expected that the resonances for the corresponding methylene groups within [BBIPYXYBXY]$^{3+}$ would also appear in this region of the spectrum, if this trication was indeed present as an intermediate. In addition, the resonance for the protons of the "alongside" hydroquinone ring in the [2]catenane emerges in this region of the spectrum. The only significant resonances which were evident in this part of the spectrum were those for the reactant [BBIPYXY]$^{2+}$ and the [2]catenane. These observations suggest that the reaction follows scenario I; *i.e.*, the rate-limiting step is the alkylation of the [BBIPYXY]$^{2+}$ dication by BBB. After this initial nucleophilic substitution has occurred, the intermediate trication [BBIPYXYBXY]$^{3+}$ is rapidly complexed by BPP34C10, and this 1:1 complex quickly gives rise to ring closure of the [BBIPYBIXYCY]$^{4+}$ component to form the [2]catenane. This rapid ring closure to form the catenane results in the equilibrium between the crown ether and the tricationic intermediate [BBIPYXYBXY]$^{3+}$ being disturbed in favor of further complex formation and recurrent self-assembly of the [2]catenane. Hence, the formation of the [2]catenane is favored by both thermodynamic (binding constant) and kinetic (ring closure) factors. These complementary effects may explain the unexpectedly high efficiency of the clipping reaction when crown ethers larger than BPP34C10 are employed in the catenations.

The size of the [BBIPYBIXYCY]$^{4+}$ cyclophane's cavity is such that only one π-electron-donating ring can be included within the π-electron deficient receptor. In order to achieve the self-assembly of polycatenanes incorporating similar building blocks, it is necessary that two macrocyclic polyether rings can be threaded simultaneously through a cyclophane. Molecular modeling indicated that, simply by replacing the bridging phenylene rings of [BBIPYBIXYCY]$^{4+}$ with 4,4′-biphenylene units, it might be possible to thread two crown ether rings simultaneously through the central cavity of this "expanded" tetracationic cyclophane. Hence, the synthesis of a range of [3]catenanes should be possible. Indeed, this objective has been realized.[24] Reaction of 1,1′-bis(bromomethyl)-4,4′-biphenyl (BBBP) with [BBIPYBT][PF_6]$_2$ in the presence of an excess of a crown ether (BPP(3*n*+4)C*n* (n = 10 and 11)) affords (Scheme 4) the corresponding {[2]-[BPP(3*n*+4)C*n*]-[BBIPY-BIBTCY]catenane} and {[3]-[BPP(3*n*+4)C*n*]-[BBIPYBIBTCY]-[BPP(3*n*+4)C*n*]catenane}s as their tetrakis(hexafluorophosphate) salts. A similar reaction, which employed BPP40C12 as the template, afforded only {[3]-[BPP40C12]-[BBIPY-BIBTCY]-[BPP40C12]catenane}$^{4+}$ in low (2%) yield. In the catenation employing BPP34C10 as the template, a [4]catenane (Figure 4), incorporating three macrocyclic polyethers threaded onto one cyclic dimer of the large cyclophane, was also isolated in very low (0.2%) yield. The most remarkable feature of these particular self-assembly processes is the selectivity displayed in favor of the formation of the [3]catenanes in relation to the [2]catenanes. The self-assembly process, which interlocks two π-electron rich crown ether rings inside one tetracationic cyclophane, requires that two π-electron-donating units are in close proximity to one another within the central cavity of the [BBIPYBIBTCY]$^{4+}$ tetracation, suggesting, perhaps, that the

(24) Ashton, P. R.; Brown, C. L.; Chrystal, E. J. T.; Goodnow, T. T.; Kaifer, A. E.; Parry, K. P.; Slawin, A. M. Z.; Spencer, N.; Stoddart, J. F.; Williams, D. J. *Angew. Chem., Int. Ed. Engl.* **1991**, *30*, 1039−1042.

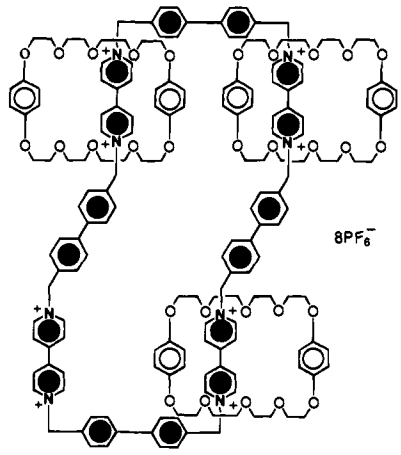

Figure 4. Structure of a [4]catenane incorporating three BPP34C10 macrocycles and one large octacationic macrocycle.

electronic character of the BPP(3*n*+4)C*n* macrocycles is altered profoundly as a result of their incorporation into the transition states associated with the ring closures that lead to the catenated structures. It is interesting to note that, in contrast with the self-assembly of the [2]catenanes, the efficiency of these [3]-catenane-forming reactions is reduced dramatically upon increasing the size of the macrocyclic polyether. This observation becomes an important consideration when the templating of the $[BBIPYBIBTCY]^{4+}$ tetracation by even larger macrocyclic polyethers is contemplated. In addition, the relatively efficient (25%) self-assembly of the $\{[3\text{-}[BPP34C10]\text{-}[BBIPYBIBTCY]\text{-}[BPP34C10]catenane\}^{4+}$ is even more remarkable when one considers that the cyclophane $[BBIPYBIBTCY]^{4+}$ could be prepared in only 2% yield, regardless of whether templating threadlike molecules incorporating hydroquinone rings were present in the reaction mixture or not.

Tetrakis(*p*-phenylene)-68-crown-20 (TPP68C20), incorporating four hydroquinone residues, was viewed[25] as another potential key precursor leading to higher catenanes, since it was envisaged that catenation of this macrocycle with $[BBIPYBIBTCY]^{4+}$ would leave available π-donor rings which could then be used as templates in further catenation steps. The crown ether TPP68C20 was prepared according to Scheme 5. However, despite repeated attempts, the self-assembly of $\{[3]\text{-}[TPP68C20]\text{-}[BBIPYBIBTCY]\text{-}[TPP68C20]catenane\}^{4+}$ proved elusive, presumably because of the flexibility and hence inferior preorganization of TPP68C20, compared with the considerable degree of preorganization present in the smaller crown ethers. In addition, TPP68C20 is rather insoluble in the solvent systems generally used for these catenations. Nonetheless, reaction (Scheme 6) of $[BBIPYXY][PF_6]_2$ with BBB in the presence of TPP68C20 at ambient pressure afforded the corresponding $\{[2]\text{-}[TPP68C20]\text{-}[BBIPYBIXYCY]catenane\}^{4+}$ in 13% yield as its tetrakis(hexafluorophosphate) salt. When the reaction (Scheme 6) was repeated at 10 kbar with an excess of $[BBIPYXY][PF_6]_2$ and BBB, the corresponding $\{[3]\text{-}[TPP68C20]\text{-}[BBIPYBIXYCY]\text{-}[TPP68C20]catenane\}^{8+}$ was isolated after fractional crystallization, in 11% yield as its octakis(hexafluorophosphate) salt.

The failure of TPP68C20 to undergo catenation with $[BBIPYBIBTCY]^{4+}$, while, under the same conditions, BPP34C10 complied as a template to afford a catenane efficiently, led us to investigate[26] the homologous crown ether of intermediate ring size—namely, tris(*p*-phenylene)-51-crown-15 (TPP51C15)—as a possible precursor to higher catenanes. The crown ether TPP51C15 was prepared by one of the two routes outlined in Scheme 7. Reaction (Scheme 8) of $[BBIPYXY][PF_6]_2$ with BBB in the presence of TPP51C15 at ambient pressure afforded the corresponding $\{[2]\text{-}[TPP51C15]\text{-}[BBIPYBIXYCY]catenane\}^{4+}$ in 48% yield. When the reaction (Scheme 8) was repeated at 10 kbar with an excess of $[BBIPYXY][PF_6]_2$ and BBB, in addition to the [2]catenane, the corresponding $\{[3]\text{-}[BBIPYBIXYCY]\text{-}[TPP51C15]\text{-}[BBIPYBIXYCY]catenane\}^{8+}$ was isolated as its octakis(hexafluorophosphate) salt in 15% yield. In contrast with TPP68C20, the catenation of TPP51C15 with $[BBIPYBIBTCY]^{4+}$ does proceed successfully as a result of reaction (Scheme 9) of BBBP with $[BBIPYBT][PF_6]_2$ in the presence of an excess of the crown ether. From this reaction mixture $\{[3]\text{-}[TPP51C15]\text{-}[BBIPYBIBTCY]\text{-}[TPP51C15]catenane\}^{4+}$ was isolated in 3.5% yield as its tetrakis(hexafluorophosphate) salt as well as a small amount (0.7%) of the corresponding $\{[2]\text{-}[TPP51C15]\text{-}[BBIPYBIBTCY]catenane\}^{4+}$. The subsequent reaction of $\{[3]\text{-}[TPP51C15]\text{-}[BBIPYBIBTCY]\text{-}[TPP51C15]\text{-}catenane\}[PF_6]_4$ with $[BBIPYXY][PF_6]_2$ and BBB in dimethylformamide at 14 kbar for 8 days afforded $\{[4]\text{-}[BBIPYBIXYCY]\text{-}[TPP51C15]\text{-}[BBIPYBIBTCY]\text{-}[TPP51C15]\text{-}catenane\}^{8+}$ in 22% yield as its octakis(hexafluorophosphate) salt. A trace of $\{[5]\text{-}[BBIPYBIXYCY]\text{-}[TPP51C15]\text{-}[BBIPYBIBTCY]\text{-}[TPP51C15]\text{-}[BBIPYBIXYCY]\text{-}catenane\}^{12+}$ was also isolated from this reaction mixture. The reluctance of the [4]catenane to react further with $[BBIPYXY][PF_6]_2$ and BBB to afford the [5]catenane was unexpected. It suggests that a negative allosteric effect, which inhibits the catenation of the [4]catenane by a further $[BBIPYBIXYCY]^{4+}$ cyclophane, might be operating during this reaction.

Scheme 5

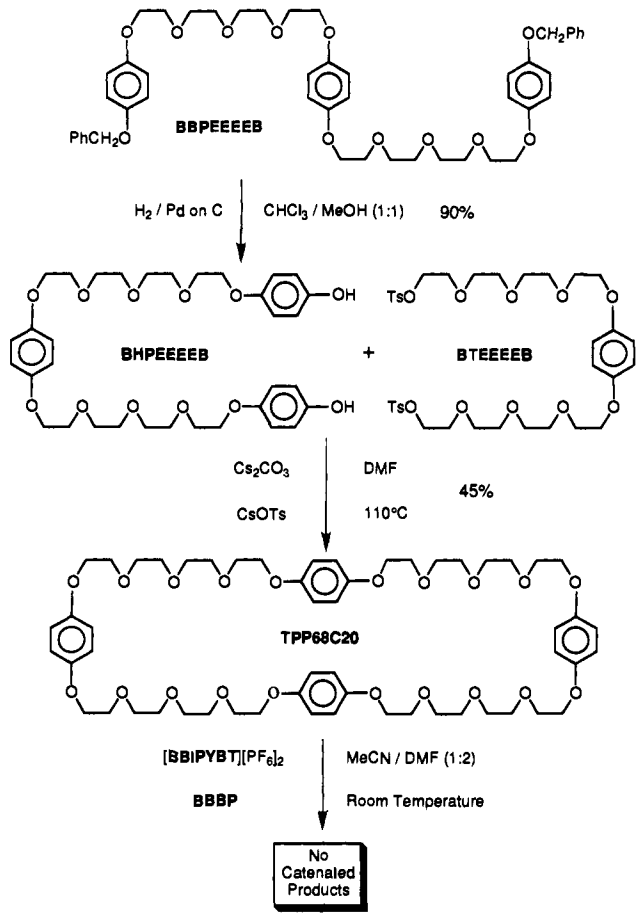

(25) Ashton, P. R.; Brown, C. L.; Chrystal, E. J. T.; Parry, K. P.; Pietraszkiewicz, M.; Spencer, N.; Stoddart, J. F. *Angew. Chem., Int. Ed. Engl.* **1991**, *30*, 1042–1045.

(26) Amabilino, D. B.; Ashton, P. R.; Reder, A. S.; Spencer, N.; Stoddart, J. F. *Angew. Chem., Int. Ed. Engl.* **1994**, *33*, 433–437.

Scheme 6

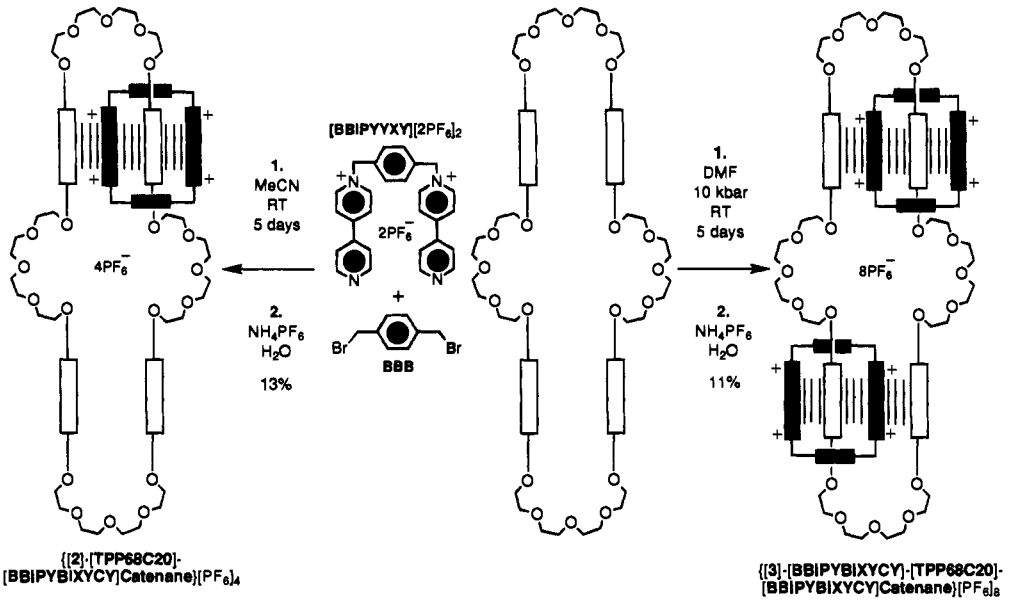

Scheme 7

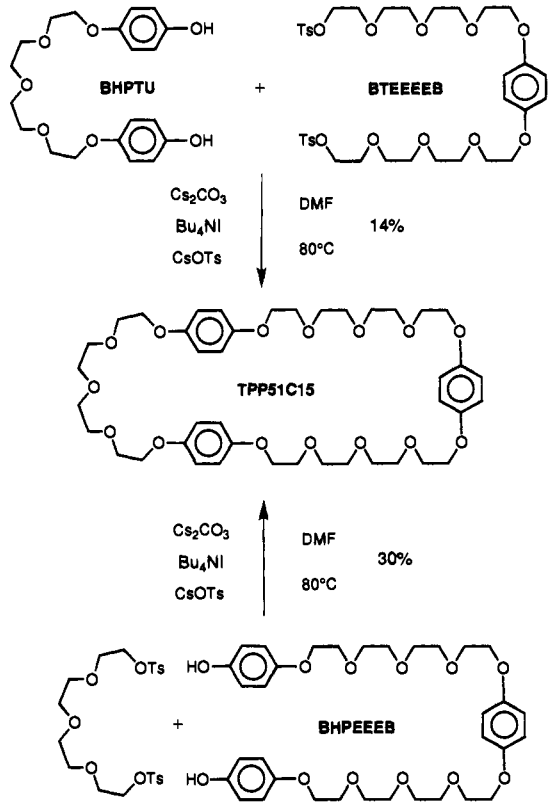

Scheme 8

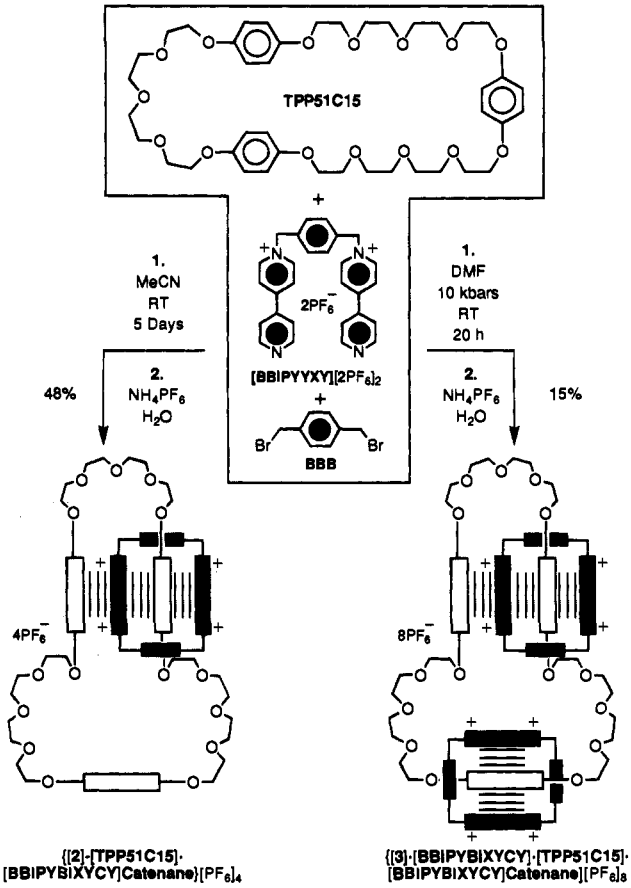

X-ray Crystal Structures. In the solid state, BPP37C11 adopts (Figure 5) an open conformation with the centroids of the two hydroquinone rings separated by 8.05 Å. Unlike BPP34C10, which is centrosymmetric in the crystalline state[1] with its hydroquinone rings parallel, here they are slightly inclined (interplanar angle 16°) and sheared such that the mean interplanar separation is reduced to 6.02 Å (*cf.* 7.20 Å in BPP34C10). A notable feature of BPP37C11 in the solid state is that, whereas one of the $-CH_2OC_6H_4OCH_2-$ units retains a normal all-planar conformation,[27] the other exhibits a distinct out-of-plane twist (70°) of one of the $O-CH_2$ bonds. Despite these conformational features, there is still a significant free pathway through the center of the macrocycle, leaving it sufficiently preorganized to permit the insertion of a π-electron deficient aromatic ring system between the two π-electron rich hydroquinone rings (*vide infra*). Analysis of the packing of the molecules in the crystal reveals important intermolecular stabilizing interactions. There are a series of C−H···π interactions (Figure 6) between the (aryloxy)methylene hydrogen atoms and the faces of both phenylene rings within the

(27) The CH_2O-aromatic unit prefers a planar arrangement. For a discussion of this conformational preference, see: Mersh, J. D.; Sanders, J. K. M.; Matlin, S. A. *J. Chem. Soc., Chem. Commun.* **1983**, 306–307.

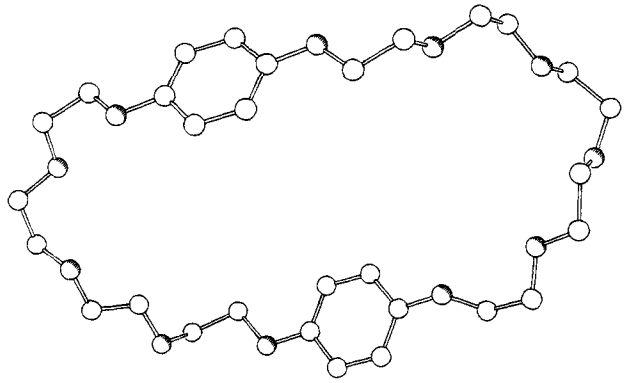

Figure 5. Ball-and-stick representation of the solid state structure of BPP37C11.

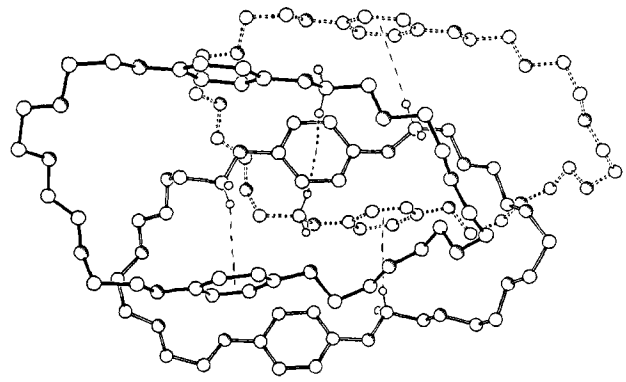

Figure 6. Ball-and-stick representation of the packing of BPP37C11 molecules in its crystals.

Scheme 9

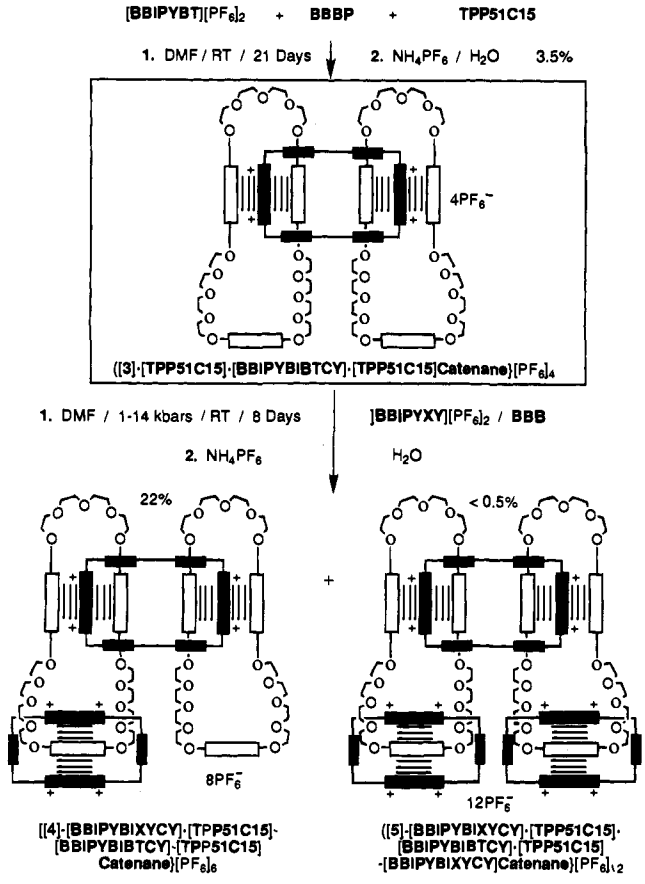

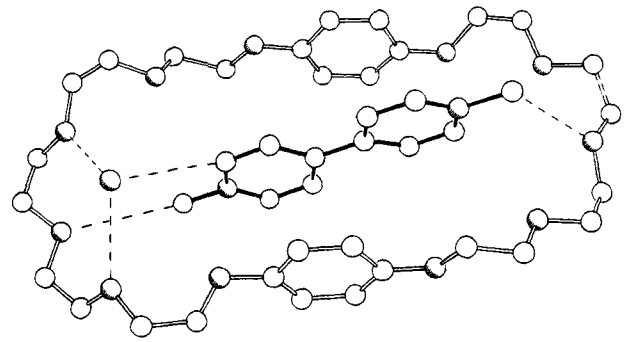

Figure 7. Ball-and-stick representation of the solid state structure of the $[PQT{\cdot}BPP37C11{\cdot}H_2O]^{2+}$ complex.

BPP37C11 molecule (the C−H···centroid distances are 2.95 and 2.99 Å). These interactions[28] extend through the crystal lattice in a cascadelike fashion, in some instances involving C−H···π interactions from both faces of a single phenylene ring.

The solid state structure (Figure 7) of the 1:1:1 complex formed among BPP37C11, the $[PQT]^{2+}$ dication, and an H_2O molecule shows that the dication is inserted through the center of the macrocycle with the π-electron deficient bipyridinium ring system sandwiched between the almost parallel (interplanar angle 1.4°) π-electron rich hydroquinone rings.[29] The mean interplanar separations between the bipyridinium dication and hydroquinone residues are 3.43 and 3.58 Å. The bipyridinium unit is nonplanar, there being a *ca.* 9° twist about the aryl−aryl bond. Also, it has its N^+-N^+ axis lying close to the plane of BPP37C11 as a consequence of C−H···O hydrogen-bonding interactions (C−O distances 3.25 and 3.48 Å) between both terminal methyl groups and polyether chain oxygen atoms at opposite sides of the macrocycle. On complexation, there is clearly a reduction in the out-of-plane rotation of the *anti*-disposed (aryloxy)methylene units, the maximum out-of-plane rotation being *ca.* 35° (*cf.* 70° in the free macrocycle). The H_2O molecule is accommodated within the arc of the longer polyether loop, and lies just above the rim of the macrocycle. It is held in position by hydrogen bonds to two of the polyether oxygen atoms (O···O 2.86 Å) and from one of the α-bipyridinium centers (C−H···O 3.33 Å). Inspection of the packing of the 1:1:1 complex in the crystal reveals (Figure 8) significant intermolecular interactions. As in the free BPP37C11, these interactions involve C−H···π hydrogen bonds,[28] though, in this case, they utilize the β-OCH_2 hydrogen atoms as opposed to the α-OCH_2 ones. The H···ring centroid distances are 2.8 and 2.9 Å, indicating the existence of cooperative intercomplex stabilizing forces that extend through the crystal *via* unit cell translations in the *b* direction. In addition to its role in strengthening the intramolecular complex, the H_2O molecules link adjacent C−H···π-bonded chains in a stepwise fashion by means of C−H···O hydrogen bonds (3.32 and 3.43 Å) from two β-bipyridinium centers (Figure 8b).

The single crystal X-ray analysis (Figure 9) of {[2]-[BPP37C11]-[BBIPYBIXYCY]catenane}$[PF_6]_4$ reveals a molecular structure with a geometry remarkably similar to its

(28) For a review on aliphatic CH−π interactions, see: Nishio, M.; Hirota, M. *Tetrahedron* **1989**, *45*, 7201−7245. For a recent example, see: Kobayashi, K.; Asakawa, Y.; Kikuchi, Y.; Toi, H.; Aoyama, Y. *J. Am. Chem. Soc.* **1993**, *115*, 2648−2654. For examples of N−H−π and OH−π interactions, see: Bakshi, P. K.; Linden, A.; Vincent, B. R.; Roe, S. P.; Adhikesavalu, D.; Cameron, T. S.; Knop, O. *Can. J. Chem.* **1994**, *72*, 1273−1293.

(29) For discussions concerning $\pi-\pi$ stacking interactions and charge transfer, see: (a) Schwarz, M. H. *J. Inclusion Phenom.* **1990**, *9*, 1−35. (b) Hunter, C. A.; Sanders, J. K. M. *J. Am. Chem. Soc.* **1990**, *112*, 5525−5534. (c) Hunter, C. A. *Chem. Soc. Rev.* **1994**, *23*, 101−109.

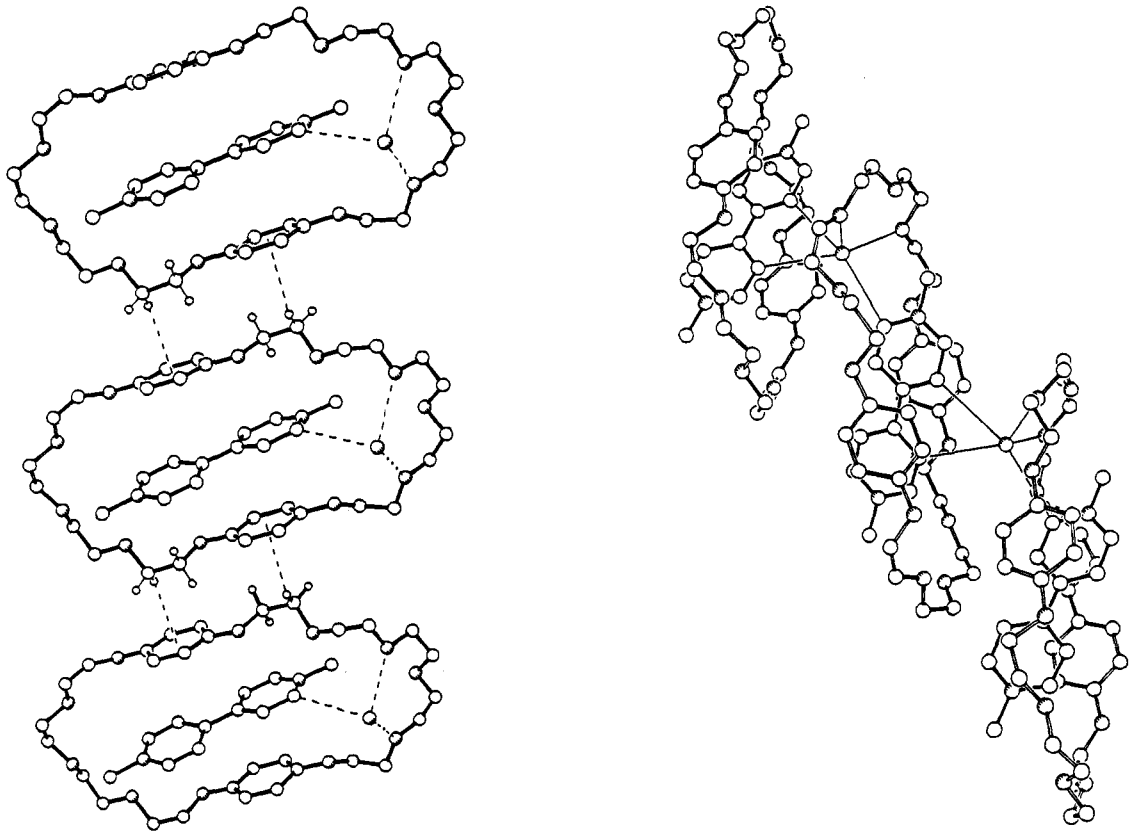

Figure 8. Ball-and-stick representations of the supramolecular structure of the $[PQT{\cdot}BPP37C11{\cdot}H_2O]^{2+}$ complex in the crystal showing (a, left) the continuous stack of the complexes in the crystal and (b, right) the binding of the water molecule to independent stacks of the complexes in the crystal.

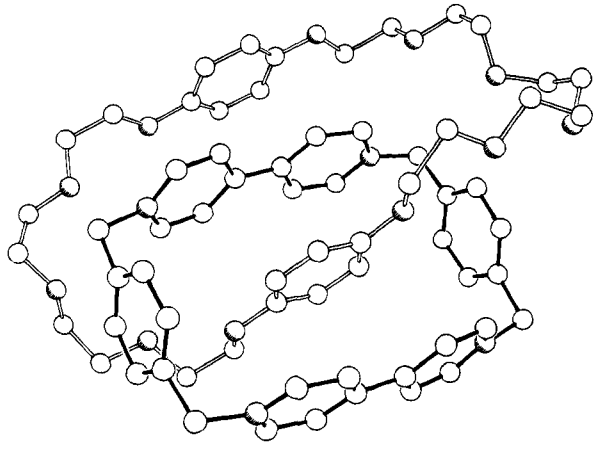

Figure 9. Ball-and-stick representation of the solid state structure of {[2]-[BPP37C11]-[BBIPYBIXYCY]catenane}$^{4+}$.

BPP34C10 counterpart.[12] However, whereas in {[2]-[BPP34C10]-[BBIPYBIXYCY]catenane}$[PF_6]_4$, the alongside $-CH_2OC_6H_4-OCH_2-$ unit adopts a *syn* geometry, here both the inside and alongside units have *anti* geometries.[30] The O−O vector associated with the inside hydroquinone residue is inclined by *ca.* 49° to the mean plane of the cyclophane which displays a characteristic barrellike distortion. The angle subtended by the CH_2-N^+ bonds of the inside bipyridinium unit is 26°, and that for the alongside bipyridinium unit is 22°. Each bipyridinium unit is also slightly twisted about its central C−C bond with mean twist angles of *ca.* 4° and *ca.* 2° for the inside and alongside units, respectively. The angles at the four methylene "corners" retain near-tetrahedral geometries with N^+-C-C angles in the range 105−107°. The overall dimensions of the tetracationic cyclophane are *ca.* 7.0 Å by *ca.* 10.2 Å. The mean interplanar separations between the inside hydroquinone ring and the two bipyridinium units are *ca.* 3.5 Å, while the alongside hydroquinone ring approaches more closely at *ca.* 3.4 Å. The centroid−centroid separations between the orthogonally-disposed inside hydroquinone ring of BPP37C11 and the *p*-xylyl residues of the cyclophane are 5.1 and 5.2 Å with, respectively, approaches of 2.75 and 2.85 Å by electropositive hydrogen atoms attached to the hydroquinone residue.[31] It is interesting to note that the *p*-xylyl centroid−hydroquinone centroid−*p*-xylyl centroid vectors subtend an angle of 179°; *i.e.*, the hydroquinone residue is precisely in the center of the cyclophane. In addition to the comparatively short contacts between the polyether oxygen atoms and both methine and methylene hydrogen atoms in the cyclophane observed previously[1] in the BPP34C10 homologue, there is a short trigonal contact (3.05 Å) between one of the electropositive α-bipyridinium carbon atoms and one of the β-oxygen atoms in the shorter polyether chain. The catenane molecules pack to form polar stacks of π-donors and π-acceptors that extend in the crystallographic *b* direction (Figure 10), the planes of the lattice translated alongside hydroquinone and alongside bipyridinium units being separated by *ca.* 3.5 Å. Adjacent stacks of opposite polarities

(30) The conformation where both $CH_2OC_6H_4OCH_2$ units are *anti* is also present in crystals of another [2]catenane. Amabilino, D. B.; Ashton, P. R.; Tolley, M. S.; Stoddart, J. F.; Williams, D. J. *Angew. Chem., Int. Ed. Engl.* **1993**, *32*, 1297−1301.

(31) For discussions concerning edge-to-face interactions between aromatic rings, see: (a) Burley, S. K.; Petsko, G. A. *J. Am. Chem. Soc.* **1986**, *108*, 7995−8001. (b) Jorgensen, W. L.; Severance, D. L. *J. Am. Chem. Soc.* **1990**, *112*, 4768−4774. (c) Hobza, P.; Selzle, H. L.; Schlag, E. W. *J. Am. Chem. Soc.* **1994**, *116*, 3500−3506. (d) Grossel, M. C.; Cheetham, A. K.; Hope, D. A.; Weston, S. C. *J. Org. Chem.* **1993**, *58*, 6654−6661. (e) Paliwal, S.; Geib, S.; Wilcox, C. S. *J. Am. Chem. Soc.* **1994**, *116*, 4497−4498.

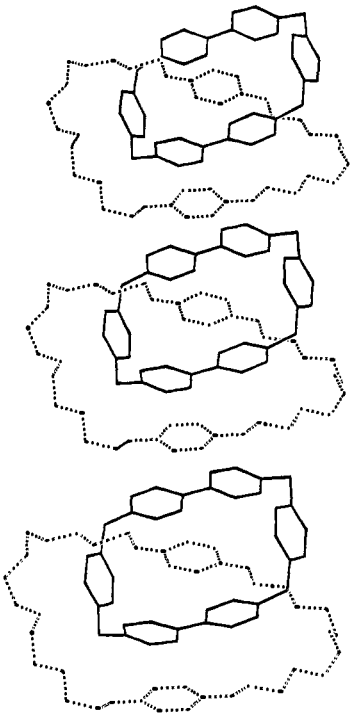

Figure 10. Part of the polar stack of {[2]-[BPP37C11]-[BBIPYBIXY-CY]catenane}$^{4+}$ in the crystal, illustrating the alternating sequence of π-electron deficient and π-electron rich aromatic moieties.

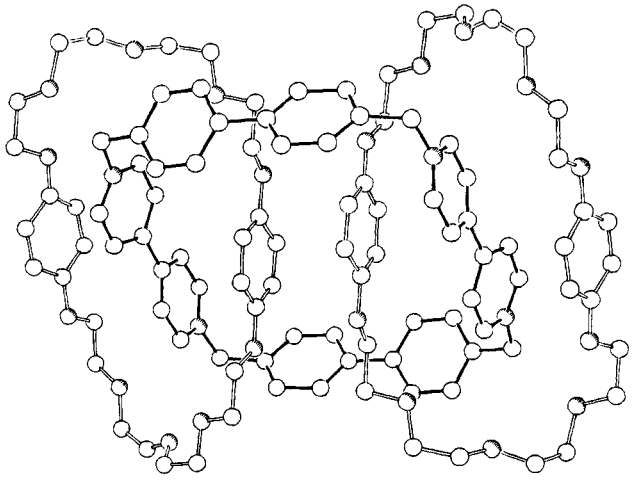

Figure 11. Ball-and-stick representation of the solid state structure of {[3]-[BPP34C10]-[BBIPYBIBTCY]-[BPP34C10]catenane}$^{4+}$.

lie parallel to each other with the *p*-xylyl rings of one stack positioned in proximity to those of another. The rings are parallel with interplanar separations of 3.8 Å and centroid–centroid distances of 4.5 Å. The arrangement is essentially identical to that observed in crystals of {[2]-[BPP34C10]-[BBIPYBIXYCY]catenane}$[PF_6]_4$. Thus, the extending of one of the polyether chains has little influence on either the molecular or supramolecular geometries in the solid state.

The X-ray crystal structure (Figure 11) of {[3]-[BPP34C10]-[BBIPYBIBTCY]-[BPP34C10]catenane}$[PF_6]_4$ shows that, as predicted from molecular modeling, the extended tetracationic cyclophane with bitolyl spacers replacing *p*-xylyl units is indeed of sufficient dimensions to permit comfortably the simultaneous threading of two hydroquinone rings through its center.[24] The inside hydroquinone residues are disposed about a center of symmetry with an interplanar separation of 3.63 Å and a centroid–centroid distance of 3.82 Å. They are both tilted with their O–O vectors inclined by 49° to the plane of the

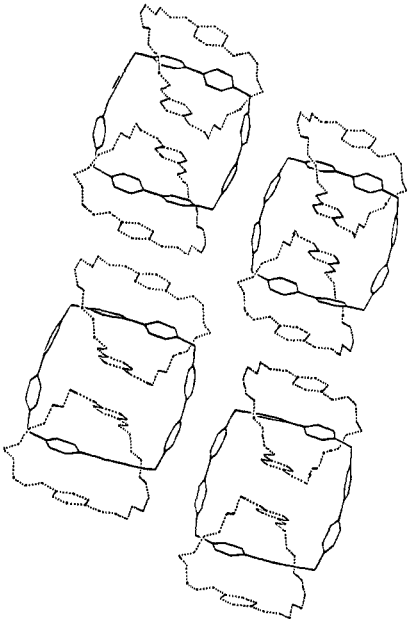

Figure 12. Part of the continuously stacked array of {[3]-[BPP34C10]-[BBIPYBIBTCY]-[BPP34C10]catenane}$^{4+}$ in the crystal.

cyclophane. In contrast with the [2]catenane incorporating the $[BBIPYBIXYCY]^{4+}$ cyclophane, the inside $-CH_2OC_6H_4OCH_2-$ units have a *syn* geometry, while the alongside $-CH_2OC_6H_4OCH_2-$ units have an *anti* geometry. In the former compound, these geometries are reversed. The separations between the mean planes of the bipyridinium units and the inside and alongside hydroquinone residues are 3.56 and 3.52 Å, respectively. The tetracationic macrocycle adopts a square boxlike conformation with an 18° twist angle between the two pyridinium rings of each bipyridinium unit and a 29° twist angle between the two phenylene rings of each biphenylene unit. The strain in the molecule is relieved by out-of-plane bending of the eight aromatic rings. Although the strain is distributed throughout the macrocycle, the maximum deviations are associated with the exocyclic N^+-CH_2 and $C-CH_2$ bonds emanating from the bipyridinium and biphenylene units, respectively. These bonds subtend angles of 17° and 25°, respectively. A consequence of this relief of strain in the larger cyclophane is the presence of near-normal tetrahedral angles (109° and 110°) at the four corner methylene carbon atoms; *cf.* the noticeably reduced values in {[2]-[BPP34C10]-[BBIPY-BIXYCY]catenane}$[PF_6]_4$ and its analogues. In common with the [2]catenane, there are edge-to-face interactions between the inside hydroquinone residues and the appropriately-located phenylene rings of the biphenylene units. The centroid–centroid distances for these T-type interactions are 5.03 and 5.93 Å, respectively. There are close intramolecular contacts between some of the polyether oxygen atoms and the *N*-methylene and α-bipyridinium carbon atoms within the large tetracationic cyclophane. Most notable among these is one of 3.15 Å to an *N*-methylene carbon atom and three of 3.23, 3.29, and 3.28 Å to one of the α-bipyridinium carbon atoms, the last of these involving a trigonal approach to the ether oxygen atom. An interesting feature of the ordering within the molecule is the loss of the alternating π-donor/π-acceptor sequence present in the [2]catenanes. Furthermore, this sequence extends beyond the molecule throughout the crystal (Figure 12), producing a continuously stacked array. Within this array, the mean plane separation between neighboring alongside hydroquinone rings is 3.66 Å, the centroid–centroid separation being 4.34 Å. Adjacent stacks are positioned with one phenylene ring of each

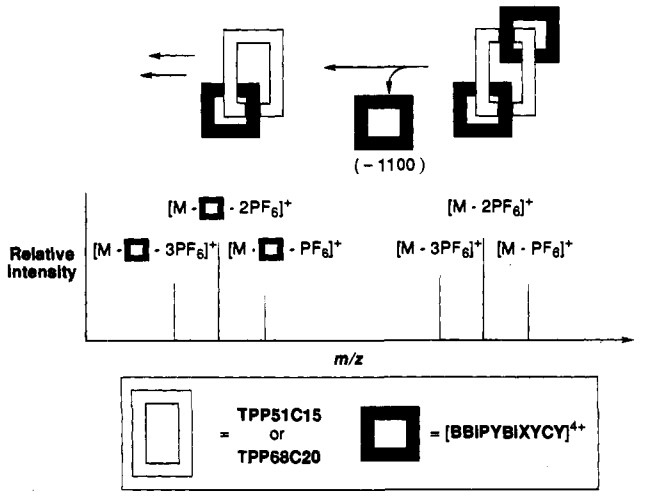

Figure 13. Schematic representation of the mass spectra of the [3]catenanes incorporating two [BBIPYBIXYCY]$^{4+}$ cyclophanes.

biphenylene unit in one stack parallel to (interplanar separation 3.60 Å, centroid−centroid distance 3.79 Å) a centrosymmetrically related one in another. These two modes of π-stacking result in the formation of a two-dimensional network of face-to-face and edge-to-face aromatic rings.

Mass Spectrometry. Soft-ionization mass spectrometric techniques[32,33] are the most convenient ones for the analysis of the catenanes described in this paper. In particular, fast atom bombardment (FAB) mass spectrometry, liquid secondary ion (LSI) mass spectrometry, and electrospray (ES) mass spectrometry have been employed. All the FAB mass spectra of the homologous series of [2]catenanes {[2]-[BPP(3n+4)Cn]-[BBIPYBIXYCY]catenane}$[PF_6]_4$ with n = 9 and 11−14 contained peaks corresponding to the $[M - PF_6]^+$, $[M - 2PF_6]^+$, and $[M - 3PF_6]^+$ ions. Occasionally, an $[M]^+$ peak was also observed. Similarly, the [3]catenanes, containing the [BBIPYBIBTCY]$^{4+}$ cyclophane, give mass spectra in which one, two, and three hexafluorophosphate counterions have been lost from the molecule. In addition, peaks are observed for the corresponding [2]catenanes (with loss of counterions), where one BPP(3n+4)Cn (n = 10−12) is cleaved and lost from the [3]-catenanes in the mass spectrometer.[34] The [4]catenane which was isolated from the reaction that formed the [3]catenane incorporating BPP34C10, namely, {[4]-1-[BPP34C10]-2-[TBIPYTBTCT-2_1-BPP34C10]-3-[BPP34C10]catenane}$[PF_6]_8$, was characterized by ES mass spectrometry,[33] which revealed peaks corresponding to the $[M - 2PF_6]^{2+}$ and $[M - 3PF_6]^{3+}$ ions. Essentially, no fragmentation was observed. {[3]-[BBIPYBIXYCY]-[TPP68C20]-[BBIPYBIXYCY]-catenane}$[PF_6]_8$ gives[25] a FAB mass spectrum in which peaks are observed for the $[M - PF_6]^+$ to $[M - 5PF_6]^+$ ions. In addition, the spectrum reveals peaks corresponding to the loss of one and two hexafluorophosphate counterions from {[2]-[TPP68C20]-[BBIPYBIXYCY]catenane}$[PF_6]_4$, commensurate with cleavage and loss of one of the tetracationic cyclophanes from the [3]catenane under the spectroscopic conditions (Figure 13).

(32) The first reports of mass spectrometry of catenanes were described by the following: (a) Vetter, W.; Schill, G. *Tetrahedron* **1967**, *23*, 3079−3093. (b) Vetter, W.; Logemann, E.; Schill, G. *Org. Mass Spectrom.* **1977**, *12*, 351−369.

(33) For a report on the characterization of similar catenated structures by electrospray mass spectrometry, see: Ashton, P. R.; Brown, C. L.; Chapman, J. R.; Gallagher, R. T.; Stoddart, J. F. *Tetrahedron Lett.* **1992**, *33*, 7771−7774. Electrospray mass spectrometry has also been used for the characterization of catenates; see ref 18c.

(34) The sequential loss of rings from catenated structures under mass spectroscopic conditions has also been noted in catenates. See: Weiss, J.; Sauvage, J.-P. *J. Am. Chem. Soc.* **1985**, *107*, 6108−6610.

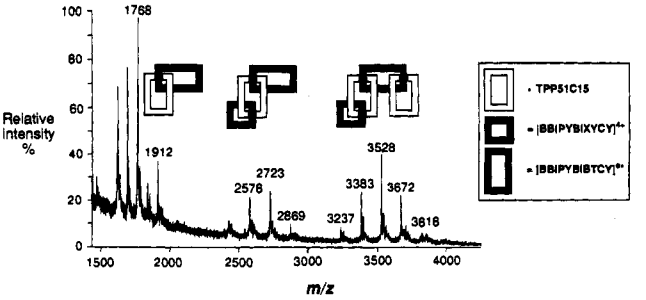

Figure 14. LSI mass spectrum of the [4]catenane.

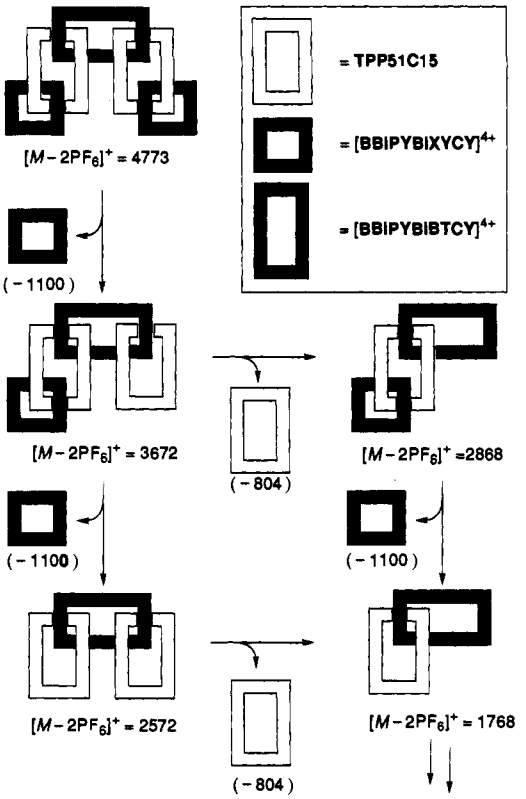

Figure 15. Fragmentation sequence of the [4]- and [5]catenanes in their LSI mass spectra. Only four significant figures are quoted. Hence, there are arithmetic anomolies.

Mass spectrometry proved to be an indispensable analytical tool in the characterization of the [4]- and [5]-catenanes and their precursors.[26] The FAB mass spectrum of {[2]-[TPP51C15]-[BBIPYBIXYCY]catenane}$[PF_6]_4$, {[3]-[BBIPYBIXYCY]-[TPP51C15]-[BBIPYBIXYCY]catenane}$[PF_6]_8$, and {[3]-[TPP51C15]-[BBIPYBIBTCY]-[TPP51C15]catenane}$[PF_6]_4$ revealed clusters of peaks similar to those of their lower homologues. The [4]- and [5]-catenanes were characterized by LSI mass spectroscopy. The spectrum of the [4]catenane gave a peak at m/z 3818, corresponding to the $[M - PF_6]^+$ ion, followed by those arising from the sequential loss of three further counterions. Cleavage and loss of macrocyclic polyether and cyclophane rings in the spectrometer resulted in peaks corresponding to {[3]-[BBIPYBIBTCY]-[TPP51C15]-[BBIPYBIXYCY]catenane}$[PF_6]_8$ and {[3]-[TPP51C15]-[BBIPYBIBTCY]-[TPP51C15]catenane}$[PF_6]_4$, respectively. The [5]catenane gives an LSI mass spectrum (Figure 14) with four peaks having m/z values between 4774 and 4338, corresponding to the loss of two to five hexafluorophosphate counterions from the parent, along with all the peaks present in the spectrum of the [4]catenane (Figure 15) which arise from decatenation in the spectrometer.

Table 1. ^{1}H NMR (400 MHz) Chemical Shift Data [δ Values ($\Delta\delta$ Values)][a] for the {[2]-[BPP(3n+4)Cn]-[BBIPYBIXYCY]-catenane}$[PF_6]_4$ Series in CD_3COCD_3 Solution

	[BBIPYBIXYCY]$^{4+}$ component[b]				crown ether component[c]	
crown ether	α-CH	β-CH	C_6H_4	CH_2N^+	ArH alongside	ArH inside
BPP31C9	9.31	8.12	8.02	6.03	6.28	3.78
	(−0.07)	(−0.46)	(+0.26)	(−0.12)	(−0.47)	(−2.97)
BPP34C10	9.28	8.18	8.04	6.01	6.22	3.76
	(−0.10)	(−0.40)	(+0.28)	(−0.14)	(−0.55)	(−3.01)
BPP37C11	9.27	8.16	8.05	6.06	6.31	3.78
	(−0.11)	(−0.42)	(+0.29)	(−0.09)	(−0.50)	(−3.03)
BPP40C12	0.25	8.16	8.05	6.05	6.34[d]	3.67[e]
	(−0.13)	(−0.42)	(+0.29)	(−0.10)	(−0.49)	(−3.16)
BPP43C13	9.30	8.18	8.02	6.06	6.84[f]	3.65[g]
3.65[g]	(−0.08)	(−0.40)	(+0.26)	(−0.09)	(−0.01)	(−3.20)
BPP46C14	9.30	8.18	8.00	6.05	6.75[h]	3.60[i]
	(−0.08)	(−0.40)	(+0.24)	(−0.10)	(−0.10)	(−3.25)

[a] The $\Delta\delta$ values indicated in parentheses under the respective δ values relate to the changes in chemical shift exhibited by the probe protons upon catenane formation. A negative value indicates a movement of the resonance to high field. [b] The δ values for the tetracationic cyclophane in CD_3COCD_3 are 9.38, 8.58, 7.76, and 6.15 for the α-CH, β-CH, C_6H_4, and CH_2N^+ protons, respectively. [c] The chemical shifts of the hydroquinone ring proton resonances in the macrocyclic polyethers BPP31C9 to BPP46C14 in CD_3COCD_3 are δ 6.78, 6.77, 6.81, 6.83, 6.85, and 6.85, respectively. [d] At 253 K. The resonance is too broad to be observed at room temperature. [e] Identified by a saturation transfer experiment performed at 253 K. [f] At 263 K. The resonance is too broad to be observed at room temperature. [g] Identified by a saturation transfer experiment performed at 263 K. [h] At 258 K. The resonance is too broad to be observed at room temperature. [i] Identified by a saturation transfer experiment performed at 258 K.

^{1}H NMR Spectroscopy. The solution state properties of the series of [2]catenanes incorporating the BPP(3n+4)Cn crown ethers and the [BBIPYBIXYCY]$^{4+}$ tetracationic cyclophane were investigated using variable temperature 400 MHz ^{1}H NMR spectroscopy in CD_3CN (for measurements above room temperature) and in CD_3COCD_3 (for measurements below room temperature). The relevant chemical shift data are summarized in Table 1, and the associated kinetic and thermodynamic properties[35] for the dynamic processes (Schemes 10 and 11) taking place within these [2]catenanes are summarized in Table 2.

The ^{1}H NMR chemical shift data suggest that the environment of the included inside hydroquinone ring within the cavity of the tetracationic cyclophane is largely unaffected by the increasing size of the macrocyclic polyether. The chemical shifts of the proton resonances for this ring are similar magnitude throughout the series from BPP31C9 (δ 3.78) to BPP46C14 (δ 3.60), though the $\Delta\delta$ values do indicate a slightly enhanced shielding of the associated protons as the size of the macrocyclic polyether is increased from BPP31C9 ($\Delta\delta$ −2.97) to BPP46C14 ($\Delta\delta$ −3.25). However, there are much greater variations in the $\Delta\delta$ values for the resonances arising from the protons associated with the alongside hydroquinone rings on increasing the macrocyclic polyether size, particularly from BPP40C12 ($\Delta\delta$ −0.49) to BPP43C13 ($\Delta\delta$ −0.01), compared with the chemical shifts of the resonances arising from the same protons in the free crown ethers. This observation suggests that the association of the alongside hydroquinone ring of the crown ether with the outer π-face of the bipyridinium units of [BBIPYBIXYCY]$^{4+}$ becomes very weak in acetone solution when the size of the macrocycle exceeds BPP40C12. The kinetic and thermodynamic parameters for passage of the macrocyclic polyether through the cavity of the tetracationic cyclophane (process I, Scheme 10), which involves exchange of the hydroquinone rings A and B between positions inside and alongside the tetracationic cyclophane, show (Table 2) that activation barriers to this process are decreased by almost 3 kcal mol^{-1} as the size of the macrocyclic polyether is increased from BPP31C9 to BPP43C13. This decrease in activation barrier is possibly a result of a weaker interaction of the alongside hydroquinone ring with the π-electron deficient macrocycle. The free energy barrier to process I in the [2]catenane incorporating BPP46C14 is greater by 0.4 kcal mol^{-1} than the free energy barrier to the same process in the analogous [2]catenane incorporating BPP43C13. The

Scheme 10

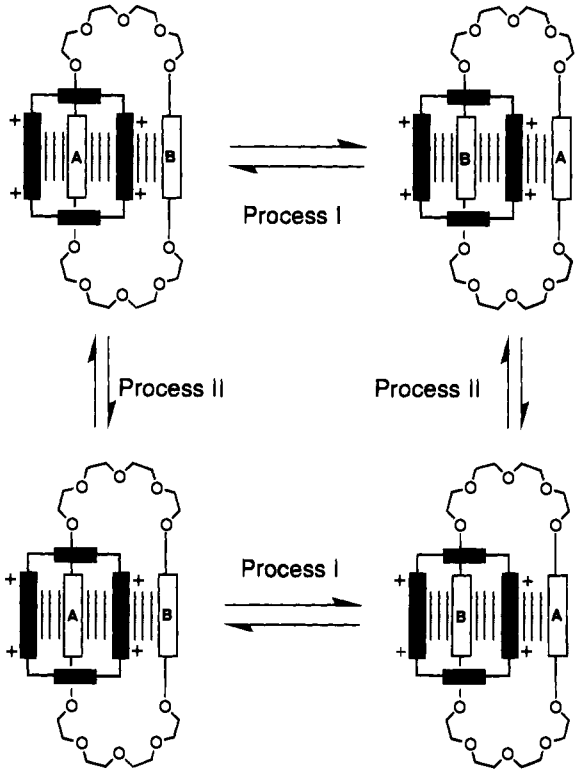

Scheme 11

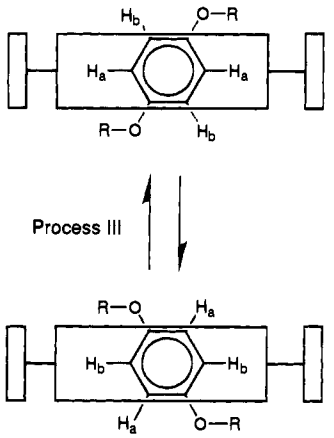

(35) The kinetic and thermodynamic data were calculated using two procedures: (a) the *coalescence method*, where values for the rate constant k_c at the coalescence temperature (T_c) were calculated (Sutherland, I. O. *Annu. Rep. NMR Spectrosc.* **1971**, *4*, 71−235) from the approximate expression $k_c = \pi(\Delta\nu)/(2)^{1/2}$, where $\Delta\nu$ is the chemical shift difference (Hz) between the coalescing signals in the absence of exchange; (b) the *exchange method*, where values of k were calculated (Sandström, J. *Dynamic NMR Spectroscopy*; Academic Press: London, 1982; Chapter 6) from the approximate expression $k = \pi(\Delta\nu)$, where $\Delta\nu$ is the difference (Hz) between the line width at a temperature T, where exchange of sites is taking place, and the line width in the absence of exchange. The Eyring equation was subsequently employed to calculate $\Delta G^{\ddagger}_c$ or $\Delta G^{\ddagger}$ values at T_c or T, respectively.

Table 2. Kinetic and Thermodynamic Parameters Obtained from the Temperature-Dependent 400 MHz ^{1}H NMR Spectra Recorded on the {[2]-[**BPP**(3*n*+4)C*n*]-[**BBIPYBIXYCY**]catenane}$[PF_6]_4$ Series

crown ether	probe protons	solvent	$\Delta\nu^a$ (Hz) ($\Delta\nu$)^b	k_c^a (s^{-1}) (k)^b	T_c^a (K) (T)^b	$\Delta G_c^{\ddagger\,a}$ (kcal mol^{-1}) ($\Delta G^{\ddagger}$)^b	process^c
BPP31C9	OC_6H_4O	CD_3CN	1092	2426	363.4	15.8	I
	C_6H_4	$(CD_3)_2CO$	72	160	253.8	12.2	II
	CH_2N^+	$(CD_3)_2CO$	44	98	252.8	12.4	II
BPP34C10	OC_6H_4O	CD_3CN	678	1505	354	15.6	I
			(19.0)	(60)	(313)	(15.7)	
	α-CH	$(CD_3)_2CO$	74.3	165	250	12.0	II
			(26.9)	(85)	(250)	(12.3)	
	β-CH	$(CD_3)_2CO$	34.3	76	247	12.2	II
			(25.1)	(79)	(247)	(12.3)	
	CH_2N^+	$(CD_3)_2CO$	45.8	102	248	12.1	II
			(30.7)	(97)	(248)	(12.2)	
BPP37C11	OC_6H_4O	$(CD_3)_2CO$	1020	2266	318.9	13.8	I
			(23)	(56.5)	(280.7)	(14.1)	
	α-CH	$(CD_3)_2CO$	16	35.5	258.5	13.2	II
			(5.4)	(17)	(258.5)	(13.6)	
	β-CH	$(CD_3)_2CO$	64	142	273	13.2	II
BPP40C12	OC_6H_4O	$(CD_3)_2CO$	1068	2372	299.1	12.9	I
	C_6H_4	$(CD_3)_2CO$	136	302	203.1	9.4	III
BPP43C13	OC_6H_4O	$(CD_3)_2CO$	1280	2843	304.5	13.0	I
	α-CH	$(CD_3)_2CO$	24	53.0	256.5	12.9	II
	β-CH	$(CD_3)_2CO$	40	88.9	265.3	13.1	II
	C_6H_4	$(CD_3)_2CO$	34	75.5	252.9	12.5	II
BPP46C14	OC_6H_4O	$(CD_3)_2CO$	1348	2994	313.1	13.4	I
			(76)	(238.8)	(284.9)	(13.6)	
	C_6H_4	$(CD_3)_2CO$	112	352	204.5	9.4	III

^{a} Data not in parentheses relate to the coalescence method (see ref 35). ^{b} Data in parentheses relate to the exchange method (see ref 35). ^{c} The dynamic processes taking place in these [2]catenanes are depicted in Schemes 10 and 11.

[2]catenane incorporating BPP46C14 also displays an alongside hydroquinone proton resonance (δ 6.75) at higher field than the corresponding proton resonance (δ 6.84) for the [2]catenane incorporating BPP43C13. These data suggest that the excluded hydroquinone ring in the [2]catenane incorporating BPP46C14 exhibits a stronger alongside interaction with the sandwiched bipyridinium unit than this same residue does in the lower homolog. This hypothesis is supported by the higher yield of the catenane containing the larger macrocycle which is compatible with more efficient templating of the [BBIPYBIXYCY]$^{4+}$ component to form the [2]catenane. However, all these observations suggest that the dominant factor influencing the magnitude of the activation barrier for process I is the strength of the interactions between the inside hydroquinone ring and the [BBIPYBIXYCY]$^{4+}$ tetracationic cyclophane. Interestingly, the free energies of activation for process I in the [2]catenanes incorporating BPP40C12 and BPP43C13 are of magnitudes similar to that of the barrier associated with the "shuttling" process in a [2]rotaxane[36] incorporating two equivalent hydroquinone "stations", separated by a tetraethylene glycol chain, and the same tetracationic cyclophane. Both activation barriers are approximately 13 kcal mol^{-1}. This observation suggests that the alongside contributions of the hydroquinone rings in the [2]catenanes incorporating the macrocyclic polyethers BPP40C12 and BPP43C13 are comparable with the same contribution present in the [2]rotaxane containing the hydroquinone rings as part of an acyclic dumbbell component.

The motion (process II, Scheme 10) of the tetracationic cyclophane through the cavities of the neutral macrocyclic polyethers in the [2]catenanes, which involves exchange of the bipyridinium units A and B between positions inside and alongside the macrocyclic polyether component, is difficult to evaluate[37] on account of the complexity in the ^{1}H NMR spectra of the catenanes at low temperatures. It is also possible that other processes[38] (*e.g.*, "rocking", as shown in process III, Scheme 11) are becoming slow on the ^{1}H NMR time scale in the low temperature spectra of these [2]catenanes. The activation barrier for process II in {[2]-[BPP31C9]-[BBIPYBIXYCY]-catenane}$[PF_6]_4$ was observed, and is of a value similar to that observed for process II in the [2]catenane containing BPP34C10. Definitive characterization of process II in the series of [2]catenanes incorporating the macrocyclic polyethers BPP37C11 to BPP46C14 was not achieved. The rocking process (process III, Scheme 11) involves exchange of the protons H_a and H_b attached to the included hydroquinone ring between positions where they are directed toward the center of the benzene ring in the *p*-xylyl spacer of the cyclophane and positions where they protrude outside the π-electron deficient cavity. This process is also slowed on the ^{1}H NMR time scale for the [2]catenanes containing BPP40C12 to BPP46C14. The slowing of this temperature-dependent process is supported by the appearance of proton resonances at approximately δ 2.0 and 5.4, which correspond to the protons attached to the inside hydroquinone ring that are directed into the π-face of the *p*-xylyl spacers of the cyclophane and out of the cavity of the cyclophane, respectively.

The relevant ^{1}H NMR chemical shift data for the series of [3]catenanes incorporating the BPP(3*n*+4)C*n* macrocyclic polyethers and the [BBIPYBIBTCY]$^{4+}$ tetracationic cyclophane in CD_3COCD_3 are summarized in Table 3. The associated kinetic and thermodynamic data for the one observable dynamic

(36) Anelli, P. L.; Spencer, N.; Stoddart, J. F. *J. Am. Chem. Soc.* **1991**, *113*, 5131–5133.

(37) Calculation of the free energy barrier for process II is usually achieved from the coalescence temperature of the resonances arising from the protons in the [BBIPYBIXCY]$^{4+}$ component. The inequivalence of these protons may arise from any dissymetry in the macrocyclic polyether, as in, for example, BPP37C11.

(38) An additional process may give rise to the coalescence of the resonances arising from inequivalent protons in the [BBIPYBIXYCY]$^{4+}$ component of the catenanes. This process may be viewed as a rotation of the bipyridinium and/or the *p*-xylyl residues about the CH_2-CH_2 axes in the cyclophane, following a slight dislocation from the π-electron rich guest ring. See: Ashton, P. R.; Brown, C. L.; Chrystal, E. J. T.; Goodnow, T. T.; Kaifer, A. E.; Parry, K. P.; Philp, D.; Slawin, A. M. Z., Spencer, N.; Stoddart, J. F.; Williams, D. J. *J. Chem. Soc., Chem. Commun.* **1991**, 634–639.

Table 3. ^{1}H NMR (400 MHz) Chemical Shift Data [δ Values ($\Delta\delta$ Values)][a] for the {[3]-[BPP(3n+4)Cn]-[BBIPYBIBTCY]-[BPP(3n+4)Cn]catenane}[PF_6]$_4$ Series in CD_3COCD_3 Solution

	[BBIPYBIBTCY]$^{4+}$ component[b]			crown ether component[c]	
crown ether	α-CH	β-CH	biphenylene	CH_2N^+	ArH
BPP34C10	9.12[d]	7.85[d]	7.70/7.80[d,e]	5.88[d]	5.24[d]
	(−0.40)	(−0.92)	(+0.02/+0.07)	(−0.32)	(−1.54)
BPP37C11	9.21	7.98	7.87[f]	6.05	5.40/5.34[e]
	(−0.31)	(−0.79)	(+0.19/+0.14)	(−0.15)	(−1.41/−1.47)
BPP40C12	9.22	8.03	7.87[f]	6.06	5.46
	(−0.30)	(−0.74)	(+0.19/+0.14)	(−0.14)	(−1.37)

[a] The $\Delta\delta$ values indicated in parentheses under the respective δ values relate to the changes in chemical shift exhibited by the probe protons upon catenane formation. A negative value indicates a movement of the resonance to high field. [b] The δ values for the [BBIPYBIBTCY]$^{4+}$ component in CD_3COCD_3 are reported in the Experimental Section. [c] The δ values of the macrocyclic polyethers are reported in the Experimental Section. [d] In CD_3CN/CD_3COCD_3 (3:7 v/v) solution. [e] δ_A/δ_B for the AB system for this resonance. [f] This resonance is observed as essentially a singlet.

Scheme 12

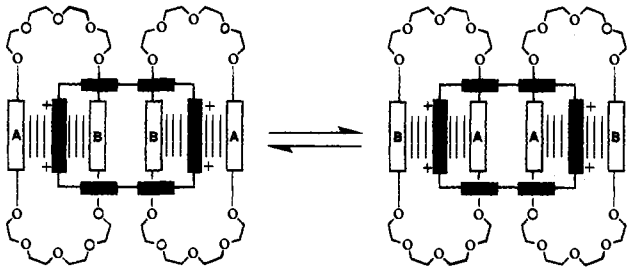

process[39] (Scheme 12) in this series of [3]catenanes are summarized in Table 4. In all of the ^{1}H NMR spectra of the [3]catenanes recorded at room temperature, a single proton resonance is observed for the hydroquinone ring protons in the macrocyclic polyether component, reflecting rapid circumrotation of the three pairs of macrocyclic polyethers (BPP34C10, BPP37C11, and BPP40C12) through the cavity of the large tetracationic cyclophane. The chemical shifts of these resonances tend to give values at lower field on increasing the size of the BPP(3n+4)Cn component, suggesting that, as noted in the case of the [2]catenanes, there is a decreased alongside interaction of the hydroquinone rings with the bipyridinium units of the tetracationic cyclophane. The activation barriers for the circumrotations of the macrocyclic polyethers through the cavity of the tetracationic cyclophane are low when compared to similar processes occurring in the [2]catenanes incorporating the smaller [BBIPYBIXYCY]$^{4+}$ and the same series of crown ethers. Presumably, this lower free energy of activation to circumrotation in the [3]catenanes is observed because the inside hydroquinone rings have a $\pi-\pi$-stacking interaction with one bipyridinium unit and the other inside hydroquinone ring, while, in the [2]catenanes incorporating the smaller tetracationic cyclophane, the inside hydroquinone ring interacts with two bipyridinium units in the cyclophane. Clearly, this situation in the [2]catenanes gives rise to stronger interactions between the components, and hence to higher activation barriers to circumrotation. As in the [2]catenanes, and in accordance with the ^{1}H NMR chemical shift data, as the size of the incorporated macrocyclic polyethers increases, the activation barrier to the circumrotation process decreases.

Tables 5 and 6 summarize the ^{1}H NMR chemical shift data as well as thermodynamic and kinetic parameters associated with the range of [2]- and [3]catenanes incorporating the macrocyclic polyethers TPP51C15 and TPP68C20, together with the [BBIPYBIXYCY]$^{4+}$ and [BBIPYBIBTCY]$^{4+}$ cyclophanes, respectively. As in the case of the homologous series of [2]catenanes incorporating [BBIPYBIXYCY]$^{4+}$, the [2]catenanes formed using both TPP51C15 and TPP68C20 as templates display ^{1}H NMR spectra where the protons attached to the inside hydroquinone rings resonate at approximately δ 3.7, while the protons on the adjacent alongside π-electron rich residues resonate between δ 6.2 and δ 6.6. In addition to these proton resonances, the [2]catenane incorporating TPP68C20 also has an "outside opposite" proton resonance at δ 6.9, a ^{1}H NMR chemical shift reminiscent of the hydroquinone ring protons in the parent macrocyclic polyether. The free energies of activation to circumrotation of the tetracationic "train" around the π-electron rich stations along the macrocyclic "track" in these "molecular train sets" (Scheme 13 illustrates the process for the [2]catenane incorporating TPP68C20) are approximately 14 kcal mol^{-1} in each case, *i.e.*, 1 kcal mol^{-1} higher than the energy barrier to the similar process in the [2]catenanes incorporating either BPP40C12 or BPP43C13. The alongside interaction of the unbound hydroquinone rings with the outside π-faces of the bipyridinium units in the tetracationic cyclophanes is weak, since the process involving rotation of the π-electron deficient component through the large macrocyclic polyether cavity (similar to process II in Scheme 10) is not slowed on the ^{1}H NMR time scale in these catenanes. The signals for the π-electron rich rings outside the cavity of the π-electron deficient cavity remain well-resolved even at very low temperatures. An alongside interaction of one of these residues would be expected to cause additional multiplicity in the resonances arising from the protons attached to them. However, in the [2]catenanes incorporating TPP51C15 and TPP68C20, the rocking process (process III in Scheme 11) of the cyclophane is frozen out on the ^{1}H NMR time scale at 188 K, as witnessed by broad resonances at approximately δ 1.9 and 5.5, corresponding to the inside hydroquinone ring protons in the two crown ethers, and by the separation into two signals of the α-CH proton resonances for the [BBIPYBIXYCY]$^{4+}$ cyclophane. It could be that coiling of the larger macrocyclic polyethers around the cyclophane, resulting in interactions of the outside hydroquinone rings with the aromatic residues of the tetracationic cyclophane, hinders both the circumrotation process and the rocking process within the cyclophane of the [2]catenanes.

When another [BBIPYBIXYCY]$^{4+}$ cyclophane is added to both TPP51C15 and TPP68C20, [3]catenanes are formed in which the free energies of activation to the circumrotation of the two tetracationic cyclophanes around the macrocyclic polyether components are significantly reduced. In the case of the [3]catenane incorporating TPP68C20 and two [BBIPYBIXYCY]$^{4+}$ cyclophanes, the activation barrier to circumrotation (Scheme 14) is reduced by approximately 0.7 kcal mol^{-1}, when compared to the results for the intermediate [2]catenane, while the corresponding reduction in activation barrier upon clipping an extra [BBIPYBIXYCY]$^{4+}$ cyclophane onto the [2]catenane, templated by TPP51C15, is approximately 1.4 kcal mol^{-1}. The free energy of activation required for the circumrotation of the two tetracationic cyclophanes around TPP51C15 can be calculated from coalescence of resonances arising from the charged components, since, when this process is slowed on the ^{1}H NMR time scale, the cyclophanes have two "sides" (Figure 16), one which "faces" the other cyclophane, and the other which faces the "outside" hydroquinone ring of the macrocyclic polyether component. The dramatic reduction in the activation barrier to circumrotation may reflect the greater

(39) Both [PQT]$^{2+}$ units of the [BBIPYBIBTCY]$^{4+}$ cyclophane are inside with respect to the cavities of the crown ethers. Therefore, only the motion of the hydroquinone rings through the cavity of the teracationic cyclophane, equivalent to Process I in Scheme 1, is observable.

Table 4. Kinetic and Thermodynamic Parameters Obtained from the Temperature-Dependent 400 MHz ^{1}H NMR Spectra Recorded on the {[3]-[BPP(3*n*+4)C*n*]-[BBIPYBIXYCY]-[BPP(3*n*+4)C*n*]catenane}$[PF_6]_4$ Series

crown ether	probe proton	$\Delta\nu^a$ (Hz) ($\Delta\nu$)^b	k_c^a (s^{-1}) (k)^b	T_c^a (K) (T)^b	$\Delta G_c^{\ddagger\,a}$ (kcal mol^{-1}) ($\Delta G^{\ddagger}$)^b	process	solvent
BPP34C10	OC_6H_4O	748	1662	248.3	10.7	I	$CD_3CN/(CD_3)_2CO$[c]
BPP37C11	OC_6H_4O	760	1688	201.4	8.6	I	$(CD_3)_2CO$
BPP40C12	OC_6H_4O	656	1457	188.7	8.1	I	$(CD_3)_2CO$

[a] Data not in parentheses relate to the coalescence method (see ref 35). [b] Data in parentheses relate to the exchange method (see ref 35). [c] 3:7 v/v.

Table 5. Chemical Shift Data [δ Values ($\Delta\delta$ Values)][a] Obtained from the 400 MHz ^{1}H NMR Spectra Recorded on the [2]- and [3]Catenanes Incorporating TPP51C15 and TPP68C20 in CD_3COCD_3 Solution

catenane type	charged component	crown ether	charged component			crown ether component	
			α-CH	β-CH	aromatic spacer[b]	CH_2N^+	ArH
[2]	BBIPYBIXYCY	TPP51C15	9.30 (−0.08)	8.15 (−0.43)	7.96 (+0.20)	6.01 (−0.14)	alongside 6.60 inside 3.75[c]
[3]	BBIPYBIXYCY	TPP51C15	9.44/9.28[d] (+0.06/−0.10)	8.37/8.18[d] (−0.21/−0.40)	8.01[d] (+0.25)	5.99[d] (−0.16)	alongside 6.32[d] inside 3.74[e]
[2]	BBIPYBIBTCY	TPP51C15	9.44 (−0.06)	8.49 (−0.28)	7.78/7.72[f] (+0.05/+0.04)	6.10 (−0.10)	6.05
[3]	BBIPYBIBTCY	TPP51C15	9.31 (−0.21)	8.13 (−0.64)	7.90/7.83[f] (+0.17/+0.15)	6.03 (−0.17)	5.99
[2]	BBIPYBIXCY	TPP68C20	9.27[g] (−0.11)	8.12[g] (−0.46)	7.97[g] (+0.21)	6.01[g] (−0.14)	outside opposite 6.91[g] outside adjacent 6.25/6.36[g] inside 3.70[h]
[3]	BBIPYBIXYCY	TPP68C20	9.15[i]	8.02[i]	7.92[i]	5.89[i]	outside 6.05[i] inside 3.45[j]

[a] The $\Delta\delta$ values indicated in parentheses under the respective δ values relate to the changes in chemical shift exhibited by the probe protons upon catenane formation. A negative value indicates a movement of the resonance to high field. [b] The aromatic spacer refers to the XY components of $[BBIPYBIXYCY]^{4+}$ and the BT components of $[BBIPYBIBTCY]^{4+}$. [c] Identified using a saturation transfer experiment performed at 263 K. [d] Values given refer to the spectrum of this compound recorded at 213 K. [e] Identified using a saturation transfer experiment carried out at 233 K. [f] δ_A/δ_B for the AB system observed for this resonance. [g] Chemical shifts are those of the resonances in the spectrum of this compound recorded at 233 K. [h] Identified using a saturation transfer experiment carried out at 273 K. [i] Spectra were measured in a 7:3 v/v mixture of CD_3COCD_3/CD_3CN. [j] Identified using a saturation transfer experiment carried out at 253 K in CD_3CN.

Table 6. Kinetic and Thermodynamic Parameters Obtained from the Temperature-Dependent 400 MHz ^{1}H NMR Spectra Recorded on the [2]- and [3]Catenanes Incorporating TPP51C15 and TPP68C20 for the Processes Depicted in Schemes 11−14

catenane type	charged component	crown ether	probe protons	solvent	$\Delta\nu^a$ (Hz) ($\Delta\nu$)^b	k_c^a (s^{-1}) (k)^b	T_c^a (K) (T)^b	$\Delta G_c^{\ddagger\,a}$ (kcal mol^{-1}) ($\Delta G^{\ddagger}$)^b	process
[2]	BBIPYBIXYCY	TPP51C15	OC_6H_4O[c]	$(CD_3)_2CO$	1116	2479	328.9	14.2	I
			OC_6H_4O[c]	CD_3CN	1244	2764	323.1	13.8	I
			β-CH	$(CD_3)_2CO$	92	204	188	8.8	III
			CH_2N^+	$(CD_3)_2CO$	92	204	188	8.8	III
[3]	BBIPYBIXYCY	TPP51C15	OC_6H_4O	$(CD_3)_2CO$	1032	2293	296.9	12.8	I
			α-CH	$(CD_3)_2CO$	60	133	259.2	12.5	I
			β-CH	$(CD_3)_2CO$	76	168.8	262.2	12.6	I
[2]	BBIPYBIBTCY	TPP51C15	OC_6H_4O[c]	$(CD_3)_2CO$	808	1795	209.2	8.9	I
[3]	BBIPYBIBTCY	TPP51C15	OC_6H_4O	$(CD_3)_2CO$	960	2133	210.6	9.0	I
[2]	BBIPYBIXYCY	TPP68C20	OC_6H_4O	$(CD_3)_2CO$	(32)	(101)	(286.5)	(14.1)	I
			α-CH	$(CD_3)_2CO$	(60)	(189)	(201)	(9.5)	III
[3]	BBIPYBIXYCY	TPP68C20	OC_6H_4O	CD_3CN	(20)	(63)	(273)	(13.7)	*d*

[a] Data not in parentheses relate to the coalescence method (see ref 35). [b] Data in parentheses relate to the exchange method (see ref 35). [c] There are two resonances (relative intensity 2:1) for the OC_6H_4O protons of TPP51C15. [d] The process observed is the passage of the TPP68C20 rings through the cavity of the $[BBIPYBIXYCY]^{4+}$ macrocycles.

steric requirements of the two tetracationic cyclophanes encircling the macrocyclic polyether, since in the [3]catenane incorporating TPP68C20, only the translational isomer depicted in Scheme 14 is observed at low temperature. Clearly, the trains prefer not to be located at adjacent stations in this [3]catenane.

The activation barrier for the observable process in the {[3]-[TPP51C15]-[BBIPYBIBTCY]-[TPP51C15]catenane}$[PF_6]_4$, where the macrocyclic polyethers circumrotate through the cavity of the large tetracationic cyclophane, is low on account of the poor organization of the incorporated large macrocyclic polyether components, in common with the analogous [3]catenanes prepared from BPP43C13 and BPP46C14. A similar free energy of activation is observed for the analogous process in {[2]-[TPP51C15]-[BBIPYBIBTCY] catenane}$[PF_6]_4$, emphasizing the weak interaction between the two included π-electron rich residues in the [3]catenane.

The room temperature ^{1}H NMR spectrum (400 MHz) (Figure 17) of the [4]catenane reflects a situation in which all the component rings are moving rapidly with respect to each other on the ^{1}H NMR time scale. As the CD_3COCD_3 solution of the [4]catenane was cooled to 193 K, all the proton resonances in the spectrum became broad, reflecting the large number of structural possibilities for this compound when equilibrations of the hydroquinone rings are "frozen out" in the cavities of the tetracationic cyclophane components on the ^{1}H NMR time scale.

Electrochemistry. The [2]catenane incorporating BPP34C10 and $[BBIPYXYCY]^{4+}$ as its components exhibits two well-

Scheme 13

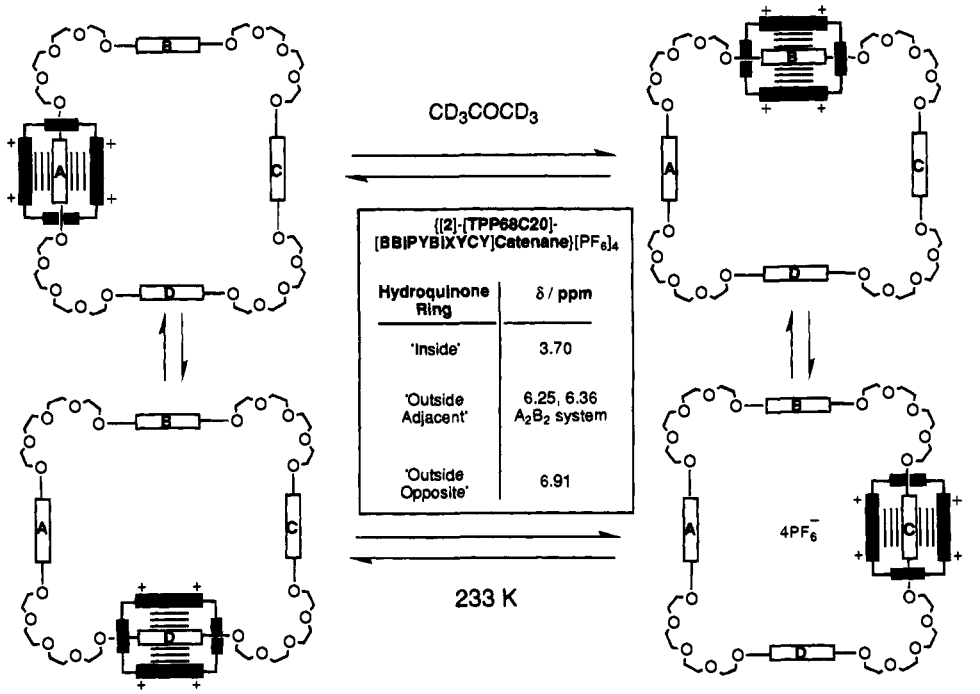

Scheme 14

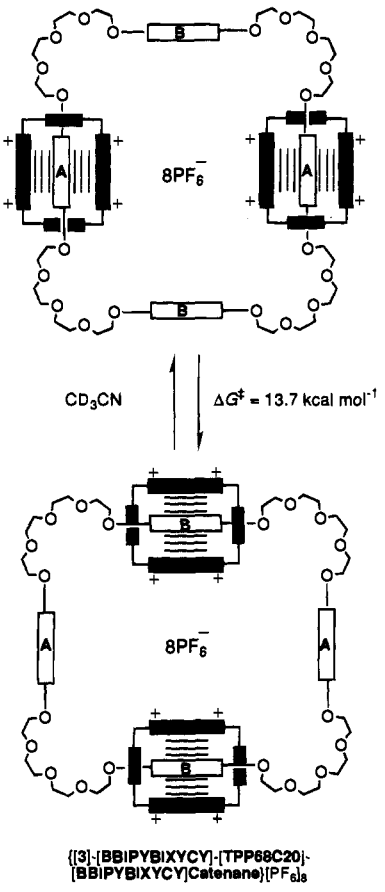

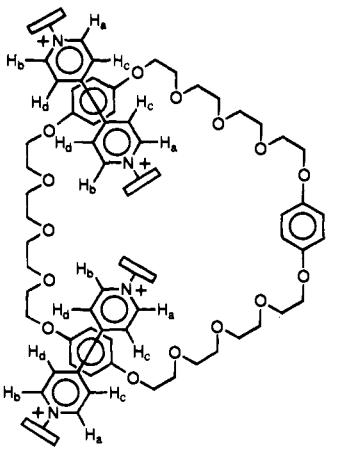

Figure 16. Structure of {[3]-[BBIPYBIXYCY]-[TPP51C15]-[BBIPYBIXYCY]catenane}$^{8+}$, showing the two nonequivalent sides of the tetracationic cyclophanes in this structure.

resolved voltammetric waves for the monoelectronic reduction of its two bipyridinium units.[12] The alongside π-electron deficient residue is reduced more easily than the inside bipyridinium unit because the latter is sandwiched between two hydroquinone rings, while the former has a $\pi-\pi$ interaction with only one π-electron rich unit. In summary, this [2]catenane displays a *gradient* of reduction potentials which is created by the unusual topology of the molecule. The homologous series of [2]catenanes formed between the various macrocyclic polyethers and [BBIPYXYCY]$^{4+}$ offered the possibility of studying the effect of the size of the neutral component upon the magnitude of the reduction potential gradient. Therefore, we decided to investigate the electrochemical behavior of this series of [2]catenanes using cyclic voltammetry (CV) and differential pulse voltammetry (DPV).

The series of [2]catenanes, incorporating the bis(*p*-phenylene)-(3*n*+4)-crown-*n* (n = 9 and 11−13) or TPP51C15 and [BBIPYXYCY]$^{4+}$ as its components, exhibit both cathodic waves, arising from the PQT^{2+}/PQT^{+} and PQT^{+}/PQT processes of the π-electron deficient residues, and anodic waves, associated with the oxidation of the hydroquinone residues. The half-wave potentials (as measured from DPV or CV data) are summarized in Table 7. The cathodic waves associated with the PQT^{2+}/PQT^{+} conversions illustrate very clearly the effects caused by increasing the size of the neutral component. In particular, the difference between the half-wave potentials for the monoelectronic reduction of the two paraquat residues decreases mono-

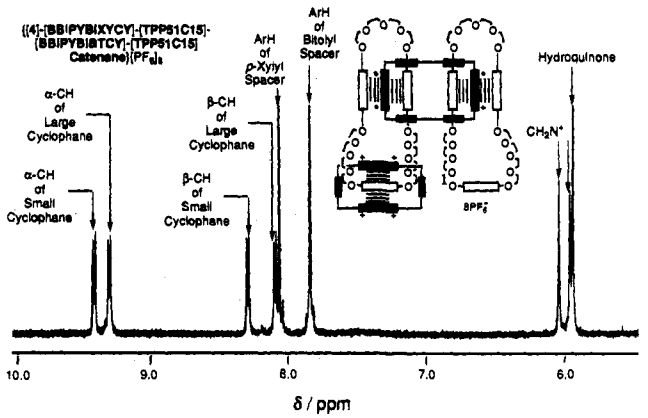

Figure 17. Partial ^{1}H NMR spectrum of the [4]catenane, illustrating the simplicity of spectra when dynamic processes are fast in catenanes of this type on the ^{1}H NMR time scale.

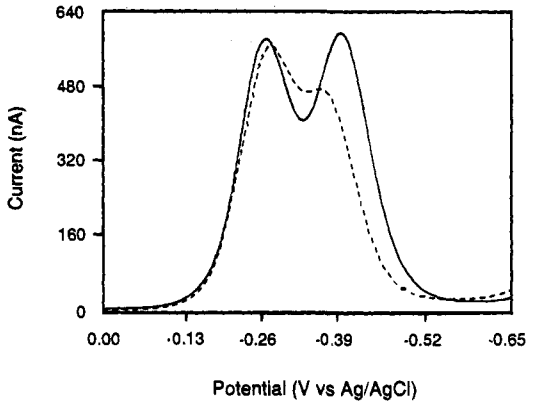

Figure 18. DPV responses on glassy carbon of 1.0 mM solutions of {[2]-[BPP31C9]-[**BBIPYBIXYCY**]catenane}$^{4+}$ (solid line) and {[2]-[BPP40C12]-[**BBIPYBIXYCY**]catenane}$^{4+}$ (dashed line) in 0.1 M [TBA][PF_6]/MeCN at 25 °C (scan rate 4 mV/s; pulse amplitude 10 mV; pulse width 50 ms).

Table 7. Voltammetric Half-Wave Potential Values (V *vs* Ag/AgCl) at 25 °C for a Series of [2]Catenanes Comprised of the [**BBIPYXYCY**]$^{4+}$ Tetracationic Cyclophane and the Indicated Macrocyclic Polyether (Solvent System 0.1 M [TBA][PF_6]/CH_3CN, Concentration of Electroactive Species 1.0 mM)

macrocyclic polyether	reduction processes			oxidation processes	
	$E^1_{1/2}$	$E^2_{1/2}$	$E^3_{1/2}$	$E^1_{1/2}$	$E^2_{1/2}$
BPP31C9	−0.290[a]	−0.404[a]	−0.820	1.430	1.680
BPP37C11	−0.285[a]	−0.385[a]	−0.813	1.419	1.713
BPP40C12	−0.297[a]	−0.372[a]	−0.825	1.371	1.660
BPP43C13	−0.297[a]	−0.362[a]	0.808	1.369	1.645
TPP51C15	−0.315		−0.803	1.550[b]	

[a] Values determined from DPV data. All other potentials determined from CV data. [b] Irreversible wave.

tonically as the size of the macrocyclic polyether increases. This trend results from the gradual shift to less negative values of the half-wave potential for the reduction of the inside paraquat residue ($E^2_{1/2}$) as the neutral component dimensions are increased. By contrast, the corresponding potential for the reduction of the alongside paraquat residue ($E^1_{1/2}$) does not change appreciably with the polyether ring size. Figure 18 presents partial DPV traces (only the cathodic region corresponding to the PQT^{2+}/PQT^+ conversions is shown) for the [2]catenanes incorporating BPP31C9 and BPP40C12 macrocycles, respectively. It is noteworthy that, while the first reduction process—for the alongside paraquat residue—takes place at similar peak potentials in the two [2]catenanes, the second reduction, which corresponds to the paraquat residue inside the cavity of the neutral component, exhibits a more negative peak potential in the BPP31C9 system. Therefore, the data indicate that, as the size of the incorporated macrocyclic polyether is increased, the relative "stabilization" of the inside paraquat residue progressively disappears and its reduction potential approaches the value observed for the alongside π-electron deficient moiety. This observation is perfectly consistent with the ^{1}H NMR spectroscopic data (*vide supra*). In particular, the upfield shift in the resonance arising from the protons attached to the alongside hydroquinone residue (caused by their close proximity to the outer face of the paraquat residues in the tetracationic cyclophane) decreases as the size of the macrocyclic polyether increases (Table 7). Clearly, as the alongside hydroquinone residue becomes less closely associated with the adjacent (inside) paraquat residue, the latter becomes less stabilized by the charge transfer from the hydroquinone ring. Therefore, the cathodic electrochemical data show that increasing the size of the macrocyclic polyether component "loosens up" the [2]catenane structure, decreasing the extent of intramolecular organization of the molecule. In fact, as the macrocyclic polyether is expanded, the alongside hydroquinone residue becomes more similar to the hydroquinone residues of the corresponding free macrocycle, while the environments of the two paraquat residues in the tetracationic cyclophane become more similar to each other.

The environmental differences between the two paraquat residues are expected to vanish in {[3]-[BPP34C10]-[BBIPYXYCY]-[BPP34C10]catenane}$[PF_6]_4$ since both paraquat residues are "sandwiched" between two hydroquinone rings. This prediction is confirmed by the voltammetric behavior of the [3]catenane, which shows only two redox couples with half-wave potentials of −0.410 and −0.840 V *vs* Ag/AgCl, respectively. The first redox couple corresponds to the uptake of one electron by each paraquat residue (PQT^{2+}/PQT^+ process), while the second redox couple results from the uptake of a second electron (PQT^+/PQT), again by both residues. The electrochemical properties of the [3]catenane are thus in agreement with the behavior expected from a system possessing two equivalent reducible subunits. Notice that the half-wave potential for the first redox couple of the [3]catenane is similar to the $E_{1/2}$ value for the monoelectronic reduction of the inside paraquat unit in the [2]catenanes in the limit of small macrocyclic polyether ring size. This observation reflects the similarity of the electronic environments between the inside paraquat residue in the more highly organized [2]catenanes and the two paraquat residues in the [3]catenane.

Conclusions

The challenge we have set for ourselves is the self-assembly of large ordered nanometer-scale structures formed in selective and highly efficient ways from relatively small molecular components, which are easily synthesized from readily available starting materials. The research reported in this paper represents our first steps toward addressing this ambitious goal.

The structures of the components of some [2]- and [3]catenanes can be tuned so as to influence the outcome of the self-assembly process that brings about the interlocking of two or three rings. Altering the size of macrocyclic polyether rings containing the π-electron rich hydroquinone residues from BPP31C9 to BPP46C14 has a profound effect on their templating actions during the formation of either the [BBIPYBIXYCY]$^{4+}$ or the [BBIPYBIBTCY]$^{4+}$ cyclophanes. In the case of both these cyclophanes, BPP34C10 is the best template, presumably because of the high degree of preorganization of the macrocyclic polyether, and also its near-perfect electronic

and steric match, which allows $\pi-\pi$ stacking with each side of any included paraquat dication as well as hydrogen bonding to protons attached to the carbon atoms α to the quaternary nitrogen center. Increasing the size of the tetracationic cyclophane component leads to a decrease in the efficiency of the self-assembly process, although it should be remembered that *three* components are being brought together in *one* step. Indeed, the [3]catenanes assembled in these template-directed reactions are isolated in much higher yields (up to 25% compared with 2%) than is the free tetracationic cyclophane when it is prepared in the absence of a template. Thus, it is easier to assemble the [BBIPYBIBTCY]$^{4+}$ cyclophane as part of the [3]catenane than it is to prepare the tetracationic cyclophane on its own. Also, while the efficiency of the production of [2]catenanes incorporating the smaller tetracationic cyclophane and *one* macrocyclic polyether is only *modestly* influenced by increasing the dimensions of the neutral component, the efficiency of the self-assembly process that leads to the [3]catenanes incorporating the larger tetracationic cyclophane and *two* macrocyclic polyethers is *dramatically* affected by the size of the crown ether. Increasing the size of the crown ethers *and* the number of hydroquinone rings they contain from BPP34C10 to TPP51C15 and then to TPP68C20 permits the templating of either one or two [BBIPYBIXYCY]$^{4+}$ cyclophanes, to form the derived [2]- or [3]catenanes at ambient and ultrahigh pressures, respectively. The macrocyclic polyether TPP68C20 failed to template the formation of the [BBIPYBIBTCY]$^{4+}$ cyclophane, presumably as a result of its relatively poor preorganization, while the smaller TPP51C15, which did act as a template, allowed the self-assembly of a [3]catenane. Employing this [3]catenane, the self-assembly of a [4]- and a [5]catenane has been achieved in a controlled manner at ultrahigh pressure. The reluctance of the [4]catenane to template the formation of one more [BBIPYBIXYCY]$^{4+}$ cyclophane might be the result of a negative allosteric effect resulting from an unfavorable secondary structure in the precursor.

The molecular recognition which is being optimized in the solution state is being guided by information obtained from the solid state. The X-ray crystal structures reported in this paper reveal the highly ordered character of the free components used to self-assemble the catenanes. They also give us structural information about the catenanes themselves, and how the interlocked molecules self-organize into ordered arrays whose packing is governed by the $\pi-\pi$ stacking, hydrogen bonding, and other electrostatic interactions that enabled the compounds to self-assemble in the first place. The progress made in this research has also been aided and abetted by recent advances in the fields of mass spectrometry and NMR spectroscopy. For the larger macrocyclic polyethers, there is an approximate correlation between the chemical yields obtained in the self-assembly processes and the energy barriers to the circumrotation processes of the macrocyclic polyethers through the [BBIPYBIXYCY]$^{4+}$ cyclophane. Therefore, the quality of mutual molecular recognition between the components during the synthesis is reflected in both the chemical yields of the [2]catenanes and the free energies of activation associated with the relative motions of their interlocked rings. This observation vindicates the approach that we advocate of studying the dynamic behavior of the interlocked structures in order to gain an understanding of self-assembly processes leading to their formation. Indeed, the correlation between the information obtained from dynamic ^{1}H NMR spectroscopy and that which has emerged from the electrochemical analyses of some of the [2]catenanes reported in this paper bodes well for the creation of molecular compounds in which the electrochemical behavior is predetermined by structure design, based on the information obtained from NMR spectroscopy.

The development of our approach to self-assembly now requires increased component programming[40]—in other words, improved intercomponent recognition. Hydroquinone residues are good templates for the formation of tetracationic cyclophanes incorporating paraquat residues, but the molecular information in our macrocyclic polyethers and tetracationic cyclophanes must be increased in order that the synthesis of the higher order catenanes, like [5]catenanes and beyond, becomes routine and highly efficient. The pieces in the *molecular meccano* set must fit together perfectly in both a steric and electronic sense. When we have achieved a sufficient level of complementarity and molecular recognition between the components, then it will be possible to assemble large structures with ease using a modular approach to their chemical synthesis. Controlling such structures using chemical,[41] electrochemical,[42] or photochemical[43] stimuli is already being addressed in numerous research laboratories. The challenge remains to turn these microscopic molecular machines into macroscopic supramolecular devices.

Experimental Section

General Methods. Solvents and reagents were purified where necessary using literature methods.[44] In particular, dimethylformamide (DMF) was distilled from calcium hydride under reduced pressure, acetonitrile (MeCN) was distilled from P_2O_5, and tetrahydrofuran (THF) was heated under reflux over reflux over Na-benzophenone ketyl and distilled under nitrogen. Sodium hydride was used as a 60% dispersion in mineral oil, which was not removed before use. Oligoethylene glycol bistosylates, BPP34C10, and [BBIPYXY][PF_6]$_2$ were prepared according to published procedures.[1] Thin-layer chromatography (TLC) was performed on aluminum or plastic plates (10 × 5 cm), coated with Merck 5735 Kieselgel 60F. Developed plates were air-dried, scrutinized under a UV lamp, and then either sprayed with cerium(IV) sulfate—sulfuric acid reagent and heated at *ca.* 100 °C or developed in an iodine vapor tank. Column chromatography was performed using Kieselgel 60 (0.040—0.063 mm mesh, Merck 9385). Melting points were determined with a Reichert hot-stage microscope or an Electrothermal 9200 melting point apparatus and are uncorrected. Reactions requiring ultrahigh pressures were carried out in Teflon vessels using a custom-built ultrahigh pressure press manufactured by PSIKA Pressure Systems Limited of Glossop, U.K. Mass spectra (MS) were obtained from Kratos MS25, Profile, or MS80RF instruments, the latter being equipped with a fast atom bombardment (FAB) facility (using a krypton or xenon primary atom beam in conjunction with a 3-nitrobenzyl alcohol matrix). FAB mass spectra were recorded in the positive ion mode at a scan speed of 30 s per decade. LSI mass spectra were recorded in the positive ion mode at a scan speed of 5 s per decade on a Kratos Concept 1H mass spectrometer (accelerating voltage 8 kV; resolution 1000) which was coupled to a Sun Sparc Station with Mach3 Software. Electrospray (ES) mass spectra were recorded in the positive ion mode at a scan speed of 10 s per decade on a VG Autospec mass spectrometer (accelerating voltage 4 kV; resolution 1000) using a mobile phase of acetonitrile. ^{1}H nuclear magnetic resonance (NMR) spectra were recorded on Bruker AC300 (300 MHz), WH400 (400 MHz), or AMX400 (400 MHz) (using the deuterated solvent as the lock and

(40) An alternative approach to the construction of catenated arrays has been illustrated in the self-assembly of a bis[2]catenane; Ashton, P. R.; Reder, A. S.; Spencer, N.; Stoddart, J. F. *J. Am. Chem. Soc.* **1993**, *115*, 5286—5287.

(41) Bissell, R. A.; Córdova, E.; Kaifer, A. E.; Stoddart, J. F. *Nature* **1994**, *369*, 133—137.

(42) Ashton, P. R.; Ballardini, R.; Balzani, V.; Gandolfi, M. T.; Marquis, D. J.-F.; Pérez-García, L.; Prodi, L.; Stoddart, J. F.; Venturi, M. *J. Chem. Soc., Chem. Commun.* **1994**, 177—180.

(43) (a) Ballardini, R.; Balzani, V.; Gandolfi, M. T.; Prodi, L.; Venturi, M.; Philp, D.; Ricketts, H. G.; Stoddart, J. F. *Angew. Chem., Int. Ed. Engl.* **1993**, *32*, 1301—1303.

(44) Perrin, D. D.; Armarego, W. L. *Purification of Laboratory Chemicals*, 3rd ed.; Pergamon Press: New York, 1988.

residual solvent or tetramethylsilane as the internal reference) spectrometers. ^{13}C NMR spectra were recorded on a Bruker AC300 (75 MHz), WH400 (100 MHz), or AMX400 (100 MHz) spectrometer using the JMOD pulse sequence (assuming $^1J_{CH} = 143$ Hz). Microanalyses were performed by the University of Sheffield and the University of Birmingham Microanalytical Services.

1,8-Bis[4-(benzyloxy)phenoxy]-3,6-dioxaoctane (BBPDO). A solution of 4-(benzyloxy)phenol (6.0 g, 30.0 mmol) in dry DMF (30 mL) was added to a suspension of NaH (1.8 g, 60% in mineral oil, 45.0 mmol) in dry DMF (70 mL) over 30 min. The mixture was stirred in a nitrogen atmosphere for an additional 20 min. A solution of triethylene glycol bistosylate (7.3 g, 16.0 mmol) in dry DMF (50 mL) was added dropwise to the mixture over 2.5 h, and the temperature was slowly raised to 80 °C. Stirring and heating were continued for 24 h. The course of the reaction was follows by TLC [silica gel, hexane–acetone (3:2)]. After the reaction was cooled to room temperature, the excess of NaH was quenched by the addition of a few drops of H_2O. The DMF was completely removed at low pressure, and the residue was partitioned between toluene (250 mL) and H_2O (70 mL). The organic phase was washed with H_2O and dried ($CaCl_2$). Evaporation of the solvent in vacuo afforded a residue which was purified by column chromatography [SiO_2, hexane–acetone (3:2)] to yield BBPDO as a white crystalline material (4.9 g, 60%): mp 106–109 °C; MS 514 (M^+); ^1H NMR ($CDCl_3$) δ 3.77 (4H, s), 3.81–3.87 (4H, m), 4.05–4.11 (4H, m), 5.02 (4H, s), 6.81–6.92 (8H, m), 7.36–7.46 (10H, m). Anal. ($C_{32}H_{34}O_6$) C, H.

1,14-Bis[4-(benzyloxy)phenoxy]-3,6,9,12-tetraoxatetradecane (BBPTT). The compound was prepared in 65% yield from pentaethylene glycol bistosylate, employing the same procedure as that described for BPPDO: pale yellow oil; MS 602 (M^+); ^1H NMR ($CDCl_3$) δ 3.64–3.76 (12H, m), 3.81–3.87 (4H, m), 5.01 (4H, s), 6.80–6.91 (8H, m), 7.27–7.43 (10H, m). Anal. ($C_{36}H_{42}O_8$) C, H.

1,17-Bis[4-(benzyloxy)phenoxy]-3,6,9,12,15-pentaoxaheptadecane (BBPPH). The compound was prepared in 72% yield from hexaethylene glycol bistosylate, employing the same procedure as that described for BBPDO: creamy solid; mp 40–42 °C; MS 646 (M^+); ^1H NMR ($CDCl_3$) δ 3.60–3.71 (16H, m), 3.73–3.79 (4H, m), 4.04–4.09 (4H, m), 5.02 (4H, s), 6.82–6.92 (8H, m), 7.31–7.44 (10H, m). Anal. ($C_{38}H_{46}O_8$) C, H.

1,8-Bis(4-hydroxyphenoxy)-3,6-dioxaoctane (BHPDO). A solution of BBPDO (4.5 g, 8.8 mmol) in $CHCl_3$–MeOH (1:1, v/v, 120 mL) was subjected to hydrogenolysis over 10% palladium on charcoal (0.45 g). After removing the catalyst by filtration, the solvent was evaporated to give BHPDO as a yellow solid (2.8 g, 96%), which was employed in the following step without further purification: mp 114–116 °C; MS 334 (M^+); ^1H NMR [$(CD_3)_2CO$] δ 3.67 (4H, s), 3.72–3.78 (4H, m), 4.00–4.04 (4H, m), 6.77 (8H, s), 7.77 (2H, s); ^{13}C NMR [$(CD_3)_2CO$] δ 68.8, 70.4, 71.3, 116.4, 116.5, 152.2, 153.1. Anal. ($C_{18}H_{22}O_6$) C, H.

1,14-Bis(4-hydroxyphenoxy)-3,6,9,12-tetraoxatetradecane (BHPTT). The compound was prepared in 99% yield from BBPTT, employing the same procedure as that described for BHPDO: pale yellow solid; mp 78–79 °C; MS 422 (M^+); ^1H NMR [$(CD_3)_2CO$] δ 3.58 (4H, s), 3.68–3.72 (8H, m), 3.75–3.79 (4H, m), 3.80–3.83 (4H, m), 6.75 (8H, s), 7.67 (2H, s); ^{13}C NMR [$(CD_3)_2CO$] δ 68.9, 70.4, 71.2, 71.3, 116.4, 116.5, 152.1, 153.1. Anal. ($C_{22}H_{30}O_8$) C, H.

1,17-Bis(4-hydroxyphenoxy)-3,6,9,12,15-pentaoxaheptadecane (BHPPH). The compound was prepared in 98% yield from BBPPH, employing the same procedure as that described for BHPDO: pale yellow oil; MS 466 (M^+); ^1H NMR [$(CD_3)_2CO$] δ 3.72–3.86 (16H, m), 3.91–3.92 (4H, m), 4.05–4.08 (4H, m), 6.68 (8H, s), 7.72 (2H, s); ^{13}C NMR [$(CD_3)_2CO$] δ 68.9, 70.4, 71.2 (3C), 71.3, 116.4, 116.6, 152.2, 153.1. Anal. ($C_{24}H_{34}O_9$) C, H.

1,4,7,10,17,20,23,26,29-Nonaoxa[10.13]paracyclophane (BPP31C9). A solution of BHPDO (1.45 g, 4.3 mmol) in dry THF (250 mL) was added over 20 min to a suspension of NaH (0.5 g, 60% in mineral oil, 12.9 mmol) in dry THF (200 mL) stirred in a nitrogen atmosphere. After an additional 30 mim, tetraethylene glycol bistosylate (2.3 g, 4.5 mmol) dissolved in dry THF (250 mL) was added over 3.5 h. The reaction mixture was refluxed then for 3 days, before being cooled to room temperature. Excess NaH was quenched by the addition of a few drops of H_2O, and then the solvent was removed in vacuo before the residue was partitioned between toluene (200 mL) and H_2O (100 mL). The organic phase was washed well with 0.5 N NaOH (50 mL), 2 N HCl (80 mL), and finally H_2O (2 × 100 mL) before being dried ($CaCl_2$). Evaporation of the solvent in vacuo afforded a residue, which was purified by column chromatography [SiO_2, hexane–acetone (1:1)] to yield BPP31C9 as a white solid (0.5 g, 24%): mp 60–62 °C; MS 492 (M^+); ^1H NMR [$(CD_3)_2CO$] δ 3.63 (12H, d), 3.75–3.78 (8H, m), 3.92–3.98 (8H, m), 6.75 (8H, d); ^{13}C NMR [$(CD_3)_2CO$] δ 68.8, 69.0, 70.3, 70.4, 71.3, 71.4, 71.6, 116.0, 116.4, 154.0. Anal. ($C_{26}H_{36}O_9$) C, H.

1,4,7,10,13,20,23,26,29,32-Decaoxa[13.13]paracyclophane (BPP34C10). A solution of BHPTU (6.05 g, 12.0 mmol) in dry DMF (100 mL) was added to a mechanically stirred suspension of Cs_2CO_3 (75.7 g, 232 mmol), CsOTs (7.42 g, 24.0 mmol), and n-Bu_4NI (1.13 g, 20.0 mmol) in dry DMF (800 mL) under nitrogen, and the temperature of the mixture was raised to 80 °C. After 1.5 h, a solution of tetraethylene glycol bistosylate (6.05 g, 12.0 mmol) and CsOTs (7.42 g, 24.0 mmol) in dry DMF (100 mL) was added to the reaction mixture during 1 h. The temperature of the reaction mixture was raised to 100 °C, and it was stirred mechanically for 4 days. The warm reaction mixture was filtered at the pump, and the solid was washed with DMF (100 mL) and CH_2Cl_2 (100 mL). Removal of the solvent in vacuo afforded a tan solid which was partitioned between water (250 mL) and toluene (200 mL). The aqueous layer was extracted with toluene (2 × 250 mL) and CH_2Cl_2 (2 × 200 mL). The combined organic layers were dried ($CaCl_2/MgSO_4$) and filtered, and the solvent was evaporated to leave a residue which was purified by column chromatography [SiO_2, acetone–hexane (1:2)] to yield BPP34C10 as a white solid (2.60 g, 40%): mp 87–88 °C (lit.[45] mp 93–93 °C); FABMS 536 (M^+); ^1H NMR ($CDCl_3$) δ 3.64–3.74 (16H, m), 3.79–3.87 (8H, m), 3.95–4.03 (8H, m), 6.76 (8H, s); ^{13}C NMR ($CDCl_3$) δ 68.2, 69.8, 70.8, 70.9, 115.6, 153.2. Anal. ($C_{28}H_{40}O_{10}$) C, H. TPP68C20 was also isolated from this reaction as a white solid (0.32 g, 5%). The analytical data for this compound were identical with those of the authentic one whose synthesis is described later on this paper.

1,4,7,10,13,20,23,26,29,32,35-Undecaoxa[13.16]paracyclophane (BPP37C11). The crown ether BPP37C11 was prepared in 14% yield from BHPTT and tetraethylene glycol bistosylate, employing the same procedure as that described for BPP31C9: white solid; mp 58–59 °C; MS 580 (M^+); ^1H NMR ($CDCl_3$) δ 3.63–3.72 (20H, m), 3.80–3.86 (8H, m), 3.98–4.06 (8H, m), 6.77 (8H, s); ^{13}C NMR [$(CD_3)_2CO$] δ 68.9, 69.0, 70.4, 71.4, 71.5, 116.3, 116.3, 154.1. Anal. ($C_{30}H_{44}O_{11}$) C, H.

1,4,7,10,13,16,23,26,29,32,35,38-Dodecaoxa[16.16]paracyclophane (BPP40C12). The crown ether BPP40C12 was prepared in 9% yield from BHPTT and pentaethylene glycol bistosylate, employing the same procedure as that described for BPP31C9: white solid; mp 64–66 °C; MS 624 (M^+); ^1H NMR ($CDCl_3$) δ 3.63–3.71 (24H, m), 3.77–3.81 (8H, m), 3.98–4.03 (8H, m), 6.78 (8H, s); ^{13}C NMR [$(CD_3)_2$-CO] δ 68.9, 70.4, 71.4, 71.5, 116.3, 154.1. Anal. ($C_{32}H_{48}O_{12}$) C, H.

1,4,7,10,13,16,23,26,29,32,35,38,41-Tridecaoxa[16.19]paracyclophane (BPP43C13). The crown ether BPP43C13 was prepared in 8% yield from BHPPH and pentaethylene glycol bistosylate, employing the same procedure as that described for BPP31C9: colorless oil; MS 668 (M^+); ^1H NMR ($CDCl_3$) δ 3.61–3.72 (28H, m), 3.78–3.83 (8H, m), 4.00–4.07 (8H, m), 6.81 (8H, s); ^{13}C NMR [$CDCl_3$] δ 68.1, 68.1, 69.8, 70.5, 70.6, 70.7, 70.8, 115.6, 115.6, 153.1. Anal. ($C_{34}H_{52}O_{13}$) C, H.

1,4,7,10,13,16,19,26,29,32,35,38,41,44-Tetradecaoxa[19.19]paracyclophane (BPP46C14). The crown ether BPP46C14 was prepared in 7% yield from BHPPH and hexaethylene glycol bistosylate, employing the same procedure as that described for BPP31C9: white solid; mp 61–63 °C; MS 712 (M^+); ^1H NMR ($CDCl_3$) δ 3.60–3.69 (40H, m), 3.79–3.83 (8H, m), 6.78 (8H, s). Anal. ($C_{36}H_{56}O_{14}$) C, H.

{[2]-[BPP31C9]-[BBIPYBIXYCY]catenane}[PF_6]$_4$. A solution of [BBIPYXY][PF_6]$_2$ (93 mg, 0.13 mmol) in dry MeCN (2 mL) was added to a stirred solution of BPP31C9 (130 mg, 0.26 mmol) in dry MeCN (2 mL) under nitrogen. A deep yellow color was formed immediately, and a solution of 1,4-bis(bromomethyl)benzene (42 mg, 0.16 mmol)

(45) Helgeson, R. C.; Tamowski, T. L.; Timko, J. M.; Cram, D. J. *J. Am. Chem. Soc.* **1977**, *99*, 6411–6418.

in dry MeCN (2 mL) was added. After the reaction mixture had been stirred at room temperature for 7 days, the solvent was removed in vacuo. The residue was dissolved in a mixture of MeOH−2 N NH_4Cl−$MeNO_2$ (7:2:1, 4 mL), and insoluble polymeric materials were removed by filtration. The residue was purified by column chromatography [SiO_2, MeOH−2 N NH_4Cl−$MeNO_2$ (7:2:1)]. The catenane-containing fractions were combined and concentrated in vacuo without heating. The residue was dissolved in H_2O (7 mL), and a saturated aqueous solution of NH_4PF_6 was added until no further precipitation occurred. The precipitate was filtered off, carefully washed with H_2O (10 mL), and dried in vacuo. Pure {[2]-[BPP31C9]-[BBIPYBIXYCY]-catenane}$[PF_6]_4$ was obtained as a red solid (0.21 g, 10%): mp >240 °C; FABMS 1448 $(M - PF_6)^+$, 1302 $(M - 2PF_6)^+$; ^1H NMR [$(CD_3)_2$-CO] δ 3.45−3.50 (2 H, m), 3.57−3.62 (2H, m), 3.67−3.72 (2H, m), 3.73−3.82 (10H, m), 3.87−4.03 (16H, m), 6.03 (8H, s), 6.24 (2H, d, J_{AB} = 7 Hz), 6.29 (2H, J_{AB} = 7 Hz), 8.02 (8H, s), 8.12 (8H, br d), 9.31 (8H, d, J = 8 Hz); ^{13}C NMR [$(CD_3)_2CO$] δ 65.7, 67.5, 67.8, 68.1, 68.2, 70.0, 70.3, 70.9, 71.4, 71.9, 72.0, 114.0, 114.1, 115.6, 126.5, 131.8, 137.8, 145.8, 147.0, 151.0, 151.3, 153.1, 153.2. Anal. ($C_{62}H_{68}N_4O_9P_4F_{24}$) C, H, N.

{[2]-[BPP37C11]-[BBIPYBIXYCY]catenane}$[PF_6]_4$. This catenane was prepared in 55% yield from BPP37C11, employing the same procedure as that described for {[2]-[BPP31C9]-[BBIPYBIXYCY]-catenane}$[PF_6]_4$: red solid; mp >250 °C; FABMS 1680 (M^+), 1535 $(M - PF_6)^+$, 1390 $(M - 2PF_6)^+$; ^1H NMR [$(CD_3)_2CO$] δ 3.48−4.02 (44H, m), 6.07 (8H, s), 6.31 (4H, br s), 8.06 (8H, s), 8.10−8.21 (8H, m), 9.31 (8H, br d); ^{13}C NMR [$(CD_3)_2CO$] 65.7, 67.9, 70.4, 71.4, 115.0, 126.6, 131.8, 137.8, 145.6, 147.1. Anal. ($C_{66}H_{76}N_4O_{11}P_4F_{24}$) C, H, N.

{[2]-[BPP40C12]-[BBIPYBIXYCY]catenane}$[PF_6]_4$. This catenane was prepared in 54% yield from BPP40C12, employing the same procedure as that described for {[2]-[BPP31C9]-[BBIPYBIXYCY]-catenane}$[PF_6]_4$: red solid; mp >250 °C; FABMS 1579 $(M - PF_6)^+$, 1434 $(M - 2PF_6)^+$; ^1H NMR (CD_3CN) δ 3.53−3.76 (40H, m), 5.75 (8H, s), 7.61 (8H, d, J = 7 Hz), 7.79 (8H, s), 8.91 (8H, d, J = 7 Hz); ^{13}C NMR [$(CD_3)_2CO$] 65.9, 68.0, 70.3, 71.0, 71.1, 71.3, 71.4, 74.4, 126.7, 131.9, 137.9, 145.6, 147.2. Anal. ($C_{68}H_{80}N_4O_{12}P_4F_{24}$) C, H, N.

{[2]-[BPP43C13]-[BBIPYBIXYCY]catenane}$[PF_6]_4$. This catenane was prepared in 40% yield from BPP43C13, employing the same procedure as that described for {[2]-[BPP31C9]-[BBIPYBIXYCY]-catenane}$[PF_6]_4$: red solid; mp >250 °C; FABMS 1768 (M^+), 1622 $(M - PF_6)^+$, 1477 $(M - 2PF_6)^+$; ^1H NMR $(CD_3)_2CO$ δ 3.51−4.02 (52H, m), 6.03 (8H, s), 7.92 (8H, s), 8.18 (8H, d, J = 7 Hz), 9.30 (8H, d, J = 7 Hz); ^{13}C NMR [$(CD_3)_2CO$] 65.9, 68.4, 70.3, 70.7, 70.9, 71.1, 71.4, 71.7, 74.4, 126.7, 131.9, 137.9, 145.9, 147.4.

{[2]-[BPP46C14]-[BBIPYBIXYCY]catenane}$[PF_6]_4$. This catenane was prepared in 49% yield from BPP47C14, employing the same procedure as that described for {[2]-[BPP31C9]-[BBIPYBIXYCY]-catenane}$[PF_6]_4$: red solid; mp >250 °C; FABMS 1667 $(M - PF_6)^+$, 1522 $(M - 2PF_6)^+$; ^1H NMR [$(CD_3)_2CO$] δ 3.35−4.07 (48 H, m), 6.04 (8H, s), 7.99 (8H, s), 8.17 (8H, d, J = 7 Hz), 9.29 (8H, d, J = 7 Hz); ^{13}C NMR [$(CD_3)_2CO$] 65.9, 68.5, 70.7, 70.9, 71.2, 71.7, 126.7, 131.9, 137.9, 145.9, 147.5.

1,1′-[4,4′-Biphenylenedimethylene]bis(4,4′-bipyridinium)Bis-(hexafluorophosphate) ([BBIPYBT][PF_6]$_2$). A solution of 4,4′-bipyridine 8.0 g, 51.2 mmol) and 4,4′-bis(bromomethyl)biphenyl (1.65 g, 4.8 mmol) in MeCN (80 mL) was heated under reflux for 3 days with stirring and protection from moisture. The resulting slurry was filtered, and the solid residue was washed with MeCN and Et_2O to afford the crude material which was dissolved in boiling H_2O (200 mL) and filtered while it was still hot. The product crystallized from the aqueous liquors on the addition of a saturated aqueous solution of NH_4PF_6 and was isolated by filtration. The crude product was purified further by recrystallization from $(Me)_2CO$ to afford [BBIPYBY][PF_6]$_2$ as a yellow solid (1.43 g, 37%): mp 151−154 °C; FABMS 637 $(M - PF_6)^+$; ^1H NMR (CD_3CN) δ 5.79 (4H, s), 7.56 (4H, d, J = 8 Hz), 7.74−7.80 (8H, m), 8.33 (4H, d, J = 7 Hz), 8.81−8.88 (8H, m); ^{13}C NMR (CD_3CN) δ 64.8, 122.9, 127.3, 129.1, 130.9, 133.6, 142.2, 146.0, 152.1, 155.7. Anal. ($C_{34}H_{28}N_4P_2F_{12}$) C, H, N.

15,24,41,50-Tetraazonia[1.0.1.0.1.0.1.0]paracyclophane Tetrakis-(hexafluorophosphate) ([BBIPYBIBTCY][PF_6]$_4$). A solution of [BBIPYBT][PF_6]$_2$ (100 mg, 0.13 mmol) and 4,4′-bis(bromomethyl)-biphenyl (52 mg, 0.15 mmol) in dry MeCN (15 mL) was stirred at room temperature for 14 days. The solvent was evaporated off to afford a yellow solid, which was taken up in $MeNO_2$ (30 mL) and filtered. The filtrate was evaporated and purified by column chromatography [SiO_2, MeOH−2 N NH_4Cl−$MeNO_2$ (7:2:1)] to yield, after counterion exchange, [BBIPYBIBTCY][PF_6]$_4$ (3 mg, 2%): mp 194 °C dec; FABMS 1107 $(M - PF_6)^+$, 962 $(M - 2PF_6)^+$, 817 $(M - 3PF_6)^+$; ^1H NMR (CD_3CN) δ 5.82 (8H, s), 7.54 (8H, d, J = 8 Hz), 7.66 (8H, d, J = 8 Hz), 8.25 (8H, d, J = 7 Hz), 8.95 (8H, d, J = 7 Hz). ^1H NMR (CD_3COCD_3) δ 6.20 (8H, s), 7.68 (8H, d, J = 8 Hz), 7.73 (8H, d, J = 8 Hz), 8.77 (8H, d, J = 7 Hz), 9.52 (8H, d, J = 7 Hz). Anal. ($C_{48}H_{40}N_4P_4F_{24}$) C, H, N.

{[3]-[BPP34C10]-[BBIPYBIBTCY]·[BPP34C10]catenane}-[PF_6]$_4$, {[2]-[BPP34C10]-[BBIPYBIBTCY]catenane}[PF_6]$_4$, and {[4]-1-[BPP34C10]-2-[TBIPYTBTCY-2$_1$-BPP34C10]-3-[BPP34C10]catenane}[PF_6]$_4$. These catenanes were prepared in 25%, 2%, and 0.2% yields, respectively, from BPP34C10, [BBIPYBT][PF_6]$_2$, and 4,4′-bis-(bromomethyl)-1,1′-biphenyl, employing the same procedure as that described for {[2]-[BPP31C9]-[BBIPYBIXYCY]catenane}[PF_6]$_4$. (i) Data for [3]-[BPP34C10]-[BBIPYBIBTCY][BPP34C10]-catenane}-[PF_6]$_4$: red solid; mp >250 °C; FABMS 2181 $(M - PF_6)^+$, 2036 $(M - PF_6)^+$; ^1H NMR [$(CD_3)_2CO/CD_3CN$, 7:3, v/v] δ 3.13 (16H, br s), 3.57−3.63 (16H, m), 3.78−3.83 (16H, m), 3.83−3.88 (16H, m), 5.25 (16H, s), 5.88 (8H, s), 7.70−7.80 (16H, m), 7.85 (8H, d, J = 7 Hz), 9.12 (8H, d, J = 7 Hz); ^{13}C NMR 65.5, 67.7, 70.3, 70.9, 71.2, 114.6, 116.4, 118.1, 126.1, 128.7, 130.9, 134.9, 141.6, 145.7, 146.5, 152.1. Anal. ($C_{108}H_{128}N_4O_{22}P_4F_{24}$) C, H, N. (ii) Data for {[2]-[BPP34C10]-[BBIPYBIBTCY]catenane}[PF_6]$_4$: red solid; mp >250 °C; FABMS 1790 (M^+), 1645 $(M - PF_6)^+$, 1500 $(M - 2PF_6)^+$; ^1H NMR [$(CD_3)_2$-CO] δ 3.47−3.53 (8H, m), 3.68−3.73 (8H, m), 3.89−3.96 (16H, m), 5.46 (8H, s), 6.05 (8H, s), 7.70 (8H, d, J = 8 Hz), 7.79 (8H, d, J = 8 Hz), 8.40 (8H, d, J = 7 Hz), 9.36 (8H, d, J = 7 Hz); ^{13}C NMR [$(CD_3)_2$-CO] 65.6, 68.0, 70.7, 71.0, 71.3, 115.1, 117.6, 127.2, 128.7, 130.8, 135.1, 141.6, 146.2, 148.3, 152.5. (iii) Data for {[4]-1-[BPP34C10]-2-[TBIPYTBTCY-2$_1$-BPP34C10]-3-[BPP34C10]catenane}[PF_6]$_4$: red solid; mp >250 °C; ESMS 1912 $(M - 2PF_6)^{2+}$, 1226 $(M - 3PF_6)^{3+}$; ^1H NMR (CD_3CN) δ 3.45−3.50 (24H, m), 3.58−3.64 (24H, m), 3.72−3.65 (48H, m), 5.91 (16H, s), 5.98 (24H, s), 7.72 (16H, d, J = 8 Hz), 7.82 (16H, d, J = 8 Hz), 7.96 (16H, d, J = 7 Hz), 8.97 (16H, d, J = 7 Hz).

{[3]-[BPP37C11]-[BBIPYBIBTCY]-[BPP37C11]catenane}[PF_6]$_4$ and {[2]-[BPP37C11]-[BBIPYBIBTCY]catenane}[PF_6]$_4$. These catenanes were prepared in 13% and 2% yields, respectively, from BPP37C11, [BBIPYBT][PF_6]$_2$, and 4,4′-bis(bromomethyl)-1,1′-biphenyl, employing the same procedure as that described for {[2]-[BPP31C9]-[BBIPYBIXYCY]catenane}[PF_6]$_4$. Data for [3]-[BPP37C11]-[BBIPYBIBTCY]-[BPP37C11]catenane}[PF_6]$_4$: red solid; mp >250 °C; FABMS 2414 (M^+), 2269 $(M - PF_6)^+$, 2124 $(M - 2PF_6)^+$; ^1H NMR (CD_3CN) δ 2.99−3.08 (8H, m), 3.19−3.27 (8H, m), 3.49−3.86 (56H, m), 5.21−5.31 (8H, m), 5.35−5.45 (8H, m), 5.75 (8H, s), 7.57 (8H, d, J = 8 Hz), 7.65−7.79 (16H, m), 8.84 (8H, d, J = 7 Hz); ^{13}C NMR (CD_3CN) 65.9, 68.1, 68.2, 70.4, 70.6, 71.3, 71.4, 71.5, 71.6, 115.1, 115.2, 118.3, 126.9, 128.9, 131.2, 135.3, 141.7, 145.8, 147.4, 152.6, 152.8. Anal. ($C_{108}H_{128}N_4O_{22}P_4F_{24}$) C, H, N. Data for {[2]-[BPP37C11]-[BBIPYBIBTCY]catenane}[PF_6]$_4$: red solid; mp >250 °C; FABMS 1832 (M^+), 1687 $(M - PF_6)^+$, 1542 $(M - 2PF_6)^+$; ^1H NMR [$(CD_3)_2CO$] δ 3.46−3.52 (4H, m), 3.53−3.57 (4H, m), 3.67−3.86 (20H, m), 3.89−3.99 (8H, m), 5.49−5.59 (8H, m), 6.11 (8H, s), 7.71−7.83 (16H, m), 8.43 (8H, d, J = 7 Hz), 9.41 (8H, d, J = 7 Hz); ^{13}C NMR [$(CD_3)_2CO$] 65.7, 68.1, 70.3, 70.7, 71.1, 71.4, 115.2, 127.6, 128.4, 130.9, 135.3, 141.6, 145.4, 147.1, 148.6, 152.7, 152.8.

{[3]-[BPP40C12]-[BBIPYBIBTCY]-[BPP40C12]catenane}[PF_6]$_4$. This catenane was prepared in 2% yield from BPP40C12, [BBIPYBT][PF_6]$_2$, and 4,4′-bis(bromomethyl)-1,1′-biphenyl, employing the same procedure as that described for {[2]-[BPP31C9]-[BBIPYBIXYCY]catenane}[PF_6]$_4$: red solid; mp >250 °C; FABMS 2525 $(M + Na)^+$ 2357 $(M - PF_6)^+$, 2212 $(M - 2PF_6)^+$; ^1H NMR [$(CD_3)_2CO$] δ 3.30−3.35 (16 H, m), 3.56−3.61 (16 H, m), 3.66−3.81 (48H, m), 5.46 (16H, s), 6.06 (8H, s), 7.86 (16H, s), 8.04 (8H, d, J = 7 Hz), 9.23 (8H, d, J = 7 Hz); ^{13}C NMR [$(CD_3)_2CO$] 67.5, 67.6, 67.8,

70.7, 70.8, 70.9, 71.1, 114.6, 114.7, 114.8, 126.6, 126.7, 128.4, 128.6, 130.8, 130.9, 131.1, 145.6.

2-(2-(2-(2-Chloroethoxy)ethoxy)ethoxy)ethanol. A mixture of tetraethylene glycol (192.0 g, 1.0 mol), dry $CHCl_3$ (200 mL), and dry pyridine (80 mL) was cooled to 0 °C, and $SOCl_2$ (119.0 g, 1.0 mol) was added during 4 h, keeping the temperature of the reaction below 10 °C. The temperature was raised to 60 °C. Stirring and heating were continued for 24 h. After cooling the reaction mixture to room temperature, $CHCl_3$ was evaporated in vacuo and the residue was extracted with H_2O (2 × 100 mL). The aqueous solution was washed with hexane (2 × 100 mL), and the crude product was extracted into toluene (5 × 100 mL). The toluene extracts were dried with $MgSO_4$, before solvent was evaporated. Vacuum distillation (104−106 °C, 0.05 mmHg) afforded 2-(2-(2-(2-chloroethoxy)ethoxy)ethoxy)ethanol as a colorless liquid (75 g, 35%): MS 213 (M^+); ^1H NMR ($CDCl_3$) δ 3.41 (1H, s), 3.60−3.79 (16H, m). ^{13}C NMR ($CDCl_3$) 42.7, 61.7, 70.4, 70.5, 70.7, 70.7, 71.4, 72.5.

1,4-Bis{2-(2-(2-(2-hydroxyethoxy)ethoxy)ethoxy)ethoxy}benzene (BHEEEEB). A solution of hydroquinone (11.0 g, 0.1 mol) in dry DMF (200 mL) was added over 30 min to a stirred suspension of K_2CO_3 (69 g, 0.5 mol) in dry DMF (200 mL) under nitrogen. After an additional 30 min, a solution of 2-(2-(2-(2-chloroethoxy)ethoxy)-ethoxy)ethanol (50.0 g, 0.2 mol) in dry DMF (200 mL) was added dropwise over 1 h, and the temperature was raised to 80 °C. Stirring and heating were continued for 3 days. After cooling to room temperature, the reaction mixture was filtered and the residue was washed with DMF (100 mL). The solvent was removed in vacuo, and the residue was partitioned between toluene (250 mL) and H_2O (150 mL). The aqueous phase was washed with toluene (2 × 150 mL). The combined organic solutions were washed with NaOH (10% aqueous, 100 mL), HCl (10%, 100 mL), and finally H_2O (2 × 200 mL). Concentration in vacuo afforded BHEEEEB as a pale yellow oil (29.1 g, 63%): FABMS 462 (M^+); ^1H NMR ($CDCl_3$) δ 3.44−3.50 (4H, m), 3.52−3.63 (24H, m), 3.70−3.76 (4H, m), 6.84 (4H, s).

1,4-Bis{2-(2-(2-(*p*-tolylsulfonyl)ethoxy)ethoxy)ethoxy)ethoxy}-benzene (BTEEEEB). Powdered 4-toluenesulfonyl chloride (3.4 g, 17.7 mmol) was added in small portions to BHEEEEB (4.0 g, 8.6 mmol) in $CHCl_3$ (20 mL) and dry pyridine (2 mL) at 0 °C. The temperature of the reaction mixture was maintained below 5 °C during the addition. After stirring for 5 h, H_2O (5 mL) was added, and the slurry was stirred for a further 3 h. The organic layer was washed repeatedly with H_2O and then dried ($MgSO_4$), and the solvent was removed under reduced pressure to afford BTEEEEB as a clear oil (4.3 g, 65%): FABMS 770 (M^+); ^1H NMR ($CDCl_3$) δ 2.43 (6H, s), 3.47−3.68 (20H, m), 3.74−3.79 (4H, m), 6.85 (6H, s), 7.44−7.48 (4H, m), 7.77−7.82 (4H, m); ^{13}C NMR ($CDCl_3$) δ 21.6, 68.1, 68.7, 69.3, 69.9, 70.6, 70.7, 70.8, 115.6, 128.0, 129.8, 133.1, 144.8, 153.1. Anal. ($C_{36}H_{50}S_2O_{14}$) C, H.

1,4-Bis{2-(2-(2-(2-(4-(benzyloxy)phenoxy)ethoxy)ethoxy)ethoxy)-ethoxy}benzene (BBPEEEEB). This compound was prepared in 90% yield from BTEEEEB, employing the same procedure as that described for BBPDO. BBPEEEEB was purified by crystallization from MeOH/acetone as a white solid: mp 93−94 °C; FABMS 826 (M^+); ^1H NMR [$(CD_3)_2CO$] δ 3.59−3.67 (16H, m), 3.76−3.81 (8H, m), 4.04−4.09 (8H, m), 5.04 (4H, s), 6.85−6.97 (12H, m), 7.31−7.49 (10H, m); ^{13}C NMR ($CDCl_3$) δ 68.1, 69.9, 70.7, 70.8, 115.6, 115.7, 115.8, 127.5, 127.9, 128.6, 137.3, 153.2. Anal. ($C_{48}H_{58}O_{12}$) C, H.

1,4-Bis{2-(2-(2-(2-(4-hydroxyphenoxy)ethoxy)ethoxy)ethoxy)-ethoxy}benzene (BHPEEEEB). This compound was prepared in 90% yield from BBPEEEEB, employing the same procedure as that described for BHPDO. BHPEEEEB was obtained as a white crystalline material; mp 77−79 °C; FABMS 669 ([M + Na]$^+$), 646 (M^+); ^1H NMR [$(CD_3)_2$-CO] δ 3.58−3.65 (16H, m), 3.73−3.78 (8H, m), 3.99−4.05 (8H, m), 6.72−6.79 (8H, m), 6.84 (4H, m), 7.89 (2H, s); ^{13}C NMR [$(CD_3)_2CO$] δ 68.8, 68.8, 70.3, 70.4, 71.2, 71.2, 71.3, 71.3, 116.2, 116.3, 116.5, 152.2, 153.1, 154.0.

1,4,7,10,13,18,21,24,27,30,35,38,41,44,47-Pentadecaoxa[13.13.13]-paracyclophane (TPP51C15). Method A. A solution of BHPTU (1.9 g, 5.0 mmol) in dry DMF (70 mL) was added to a stirred suspension of Cs_2CO_3 (16.3 g, 50.0 mmol) in dry DMF (50 mL) under nitrogen, and the temperature was raised to 60 °C. After an additional 30 min, CsOTs (3.0 g, 10.0 mmol) and *n*-Bu_4NI (0.2 g, 0.5 mmol) were added to the reaction mixture. A solution of BTEEEEB (3.9 g, 5.0 mmol) in dry DMF (80 mL) was then added over 2 h, and the temperature was raised to 80 °C. Stirring and heating were continued for 3 days. After cooling to room temperature, the reaction mixture was filtered and the residue was washed with DMF (30 mL). The solvent was removed in vacuo, and the residue was partitioned between toluene (250 mL) and H_2O (50 mL). Toluene solution was dried ($CaCl_2$) and concentrated in vacuo. The residue was purified by column chromatography [SiO_2, acetone−hexane (2.5:3)] to yield TPP51C15 as a white solid (0.55 g, 14%): mp 49−51 °C; FABMS 804 (M^+); ^1H NMR ($CDCl_3$) δ 3.12−3.23 (24H, m), 3.27−3.35 (12H, m), 4.01−4.09 (12H, m), 6.82 (12H, s); ^{13}C NMR ($CDCl_3$) δ 68.2, 69.8, 70.7, 70.8, 115.7, 153.1. Anal. ($C_{42}H_{60}O_{15}$) C, H.

Method B. The synthesis of TPP51C15 was also achieved in 30% yield from BHPEEEB and tetraethylene glycol bistosylate employing the same procedure as that described in method A. The compound afforded spectroscopic data identical to those of the compound obtained using the previous method.

{[2]-[TPP51C15]-[BBIPYBIXYCY]catenane}[PF_6]$_4$. This catenane was prepared in 48% yield from TPP51C15, employing the same procedure as that described for {[2]-[BPP31C9]-[BBIPYBIXYCY]catenane}[PF_6]$_4$: red solid; mp >250 °C; FABMS 1904 (M^+), 1759 ($M - PF_6$)$^+$, 1613 ($M - 2PF_6$)$^+$; ^1H NMR [$(CD_3)_2CO$] δ 3.50−4.10 (52H, m), 6.01 (8H, s), 6.60 (8H, br s), 7.96 (8H, s), 8.15 (8H, d, J = 7 Hz), 9.30 (8H, d, J = 7 Hz); ^{13}C NMR [$(CD_3)_2CO$] δ 65.7, 70.6, 71.3, 115.9, 126.6, 128.6, 130.5, 130.7, 131.3, 131.8, 137.7, 145.7, 147.2, 151.5. Anal. ($C_{78}H_{92}N_4O_{15}P_4F_{24}$) C, H, N.

{[3]-[BBIPYBIXYCY]-[TPP51C15]-[BBIPYBIXYCY]catenane}-[PF_6]$_8$. A solution of [BBIPYXY][PF_6]$_2$ (750 mg, 1.06 mmol), TPP51C15 (170 mg, 0.21 mmol), and 1,4-bis(bromomethyl)benzene (300 mg, 1.16 mmol) in DMF (10 mL) was subjected to ultrahigh pressure (10 kbar) for 20 h. The reaction mixture was then filtered and solvent removed in vacuo. The residue was dissolved in a mixture of MeOH−2 N NH_4Cl−DMF (4:5:2, 4 mL), and insoluble polymeric materials were removed by filtration. The residue was purified by column chromatography [SiO_2, MeOH−2 N NH_4Cl−DMF (4:5:2)]. The catenane-containing fractions were combined and evaporated in vacuo without heating. The residue was dissolved in H_2O (10 mL), and a saturated aqueous solution of NH_4PF_6 was added until no further precipitation occurred. The precipitate was filtered off, carefully washed with H_2O (10 mL), and dried in vacuo. Pure {[3]-[BBIPY-BIXYCY]-[TPP51C15]-[BBIPYBIXYCY]-[BBIPYBIXYCY]catenane}-[PF_6]$_8$ was obtained as a red solid (0.92 g, 15%): mp >250 °C; FABMS 2860 ($M - PF_6$)$^+$, 2715 ($M - 2PF_6$)$^+$, 2570 ($M - 3PF_6$)$^+$, 2425 ($M - 4PF_6$)$^+$; ^1H NMR [$(CD_3)_2CO$, 53 °C] δ 3.64−4.03 (48H, m), 4.74 (12H, br s), 6.05 (16H, s), 8.03 (16H, s), 8.22 (16H, d, J = 7 Hz), 9.32 (16H, d, J = 7 Hz); ^{13}C NMR [$(CD_3)_2CO$] δ 65.8, 67.9, 70.7, 71.2, 71.5, 114.5, 126.9, 131.9, 137.8, 145.8, 147.7, 152.1.

{[3]-[TPP51C15]-[BBIPYBIBTCY]·[TPP51C15]catenane}[P-F_6]$_4$ and {[2]-[TPP51C15]-[BBIPYBIBTCY]catenane}[PF_6]$_4$. These catenanes were prepared in 3.5% and 0.7% yields, respectively, from TPP51C15, [BBIPYBT][PF_6]$_2$, and 4,4′-bis(bromomethyl)-1,1′-biphenyl, employing the same procedure as that described (stirring for 21 days) for {[2]-[BPP31C9]-[BBIPYBIXYCY]catenane}[PF_6]$_4$. Data for [3]-[TPP51C15]-[BBIPYBIBTCY]-[TPP51C15]catenane}[PF_6]$_4$: red solid; mp >250 °C; FABMS 2861 (M)$^+$, 2716 ($M - PF_6$)$^+$, 2571 ($M - 2PF_6$)$^+$, 2425 ($M - 3PF_6$)$^+$; ^1H NMR [$(CD_3)_2CO$] δ 3.57−3.78 (96H, m), 5.99 (24H, s), 6.02 (8H, s), 7.84 (8H, d, J_{AB} = 8 Hz), 7.88 (8H, d, J_{AB} = 8 Hz), 8.13 (8H, d, J = 7 Hz), 9.31 (8H, d, J = 7 Hz); ^{13}C NMR [$(CD_3)_2CO$[65.8, 68.5, 70.5, 71.3, 71.3, 115.7, 127.3, 128.8, 131.1, 135.3, 141.6, 146.0, 148.1, 153.2. Data for {[2]-[TPP51C15]-[BBIPYBIBTCY]catenane}[PF_6]$_4$: red solid: mp >250 °C; FABMS 2056 (M^+), 1911 ($M - PF_6$)$^+$, 1766 ($M - 2PF_6$)$^+$, 1621 ($M - 3PF_6$)$^+$, 1476 ($M - 4PF_6$)$^+$; ^1H NMR [$(CD_3)_2CO$] δ 3.68−3.79 (48H, m), 6.05 (12H, s), 6.10 (8H, s), 7.70−7.80 (16H, AA′BB′ system, J_{AB} = 8.5 Hz), 8.49 (8H, d, J = 6 Hz), 9.49 (8H, d, J = 6 Hz); ^{13}C NMR [$(CD_3)_2$-CO] δ 65.8, 68.6, 70.4, 71.2, 71.3, 115.9, 127.9, 128.7, 130.8, 135.3, 141.5, 146.2, 149.2, 153.4.

{[4]-[TPP51C15]-[BBIPYBIBTCY]-[TPP51C15]-[BBIPYBIXYCY]-catenane}[PF_6]$_8$ and {[5]·[BBIPYBIXYCY]-[TPP51C15]-[BBIPY·BIBTCY]-[TPP51C15]-[BBIPYBIXYCY]catenane}[PF_6]$_{12}$. A solution of [3]-[TPP51C15]-[BBIPYBIBPCY]-[TPP51C15]catenane}[PF_6]$_4$ (41.5 mg, 0.015 mmol), [BBIPYXY][PF_6]$_2$ (51.2 mg, 0.073 mmol),

and 1,4-bis(bromomethyl)benzene (21.1 mg, 0.080 mmol) in dry DMF (7 mL) was subjected to ultrahigh pressure (11 kbar) for 5 days. Then [BBIPYXY][PF_6]$_2$ (51.2 mg, 0.073 mmol) and 1,4-bis(bromomethyl)-benzene (21.1 mg, 0.080 mmol) were added to the reaction mixture, and the ultrahigh pressure reaction (14 kbar) was continued for another 3 days, before the reaction mixture was worked up employing the same procedure as that described for {[3]-[BBIPYBIXYCY]-[TPP51C15]-[BBIPYBIXYCY]catenane}[PF_6]$_8$. Pure {[4]-[TPP51C15]-[BBIPY-BIBTCY]-[TPP51C15]-[BBIPYBIXYCY]catenane}[PF_6]$_8$ was obtained as a red solid (12.9 mg, 22%): mp >250 °C; LSIMS 3818 (M − PF_6)$^+$, 3672 (M − 2PF_6)$^+$, 3528 (M − 3PF_6)$^+$, 3383 (M − 4PF_6)$^+$, 3237 (M − 5PF_6)$^+$; ^{1}H NMR [(CD_3)$_2$CO] δ 3.50−3.95 (128H, m), 5.97 (16H, s), 5.99 (8H, s), 6.07 (8H, s), 7.82−7.88 (16H, m), 8.07 (8H, s), 8.10 (8H, d, J = 7 Hz), 8.29 (8H, d, J = 7 Hz), 9.28 (8H, d, J = 7 Hz), 9.39 (8H, d, J = 7 Hz); ^{13}C NMR [(CD_3)$_2$CO] δ 65.7, 67.8, 68.4, 70.5, 71.1, 71.3, 71.4, 114.9, 115.7, 127.0, 127.4, 128.7, 131.0, 132.0, 135.4, 137.9, 141.6, 146.0, 147.8, 148.2, 153.2. The {[5]-[BBIPYBIXYCY]-[TPP51C15]-[BBIPYBIBTCY]-[TPP51C15]-[BBIPYBIXYCY]catenane}-[PF_6]$_{12}$ is a red substance: LSIMS 4774 ([M − 2PF_6]$^+$), 4629 ([M − 3PF_6])$^+$, 4483 ([M − 4PF_6])$^+$, 4338 ([M − 5PF_6])$^+$, 3818 ([M − [BBIPYBIXYCY] − PF_6]$^+$), 3673 ([M − [BBIPYBIXYCY] − 2PF_6]$^+$), 3528 ([M − [BBIPYBIXYCY] − 3PF_6]$^+$), 3013 ([M − [BBIPY-BIXYCY] − TPP51C15 − PF_6]$^+$), 2868 ([M − [BBIPYBIXYCY] − TPP51C15 − 2PF_6]$^+$), 2723 ([M − [BBIPYBIXYCY] − TPP51C15 − 3PF_6]$^+$), 2577 ([M − [BBIPYBIXYCY] − TPP51C15 − 4PF_6]$^+$).

1,4,7,10,13,18,21,24,27,30,35,38,41,44,47,52,55,58,61,64-Icosaoxa-[13.13.13.13]tetraparacyclophane (TPP68C20). This crown ether was prepared in 45% yield from BHPEEEEB and BTEEEEB, employing the same procedure as that described for TPP51C15. TPP68C20 was obtained as a white crystalline material: mp 96−98 °C; FABMS 1095 ([M + Na]$^+$), 1072 (M$^+$); ^{1}H NMR ($CDCl_3$) δ 3.66−3.73 (32H, m), 3.79−3.84 (16H, m), 4.03−4.06 (16H, m), 6.81 (16H, s); ^{13}C NMR (CD_3Cl) δ 68.1, 69.9, 70.7, 70.8, 115.6, 153.1.

{[2]-[TPP68C20]-[BBIPYBIXYCY]catenane}[PF_6]$_4$. This catenane was prepared in 13% yield from TPP68C20, employing the same procedure as that described for {[2]-[BPP31C9]-[BBIPYBIXYCY]-catenane}[PF_6]$_4$. {[2]-[TPP68C20]-[BBIPYBIXYCY]Catenane}[PF_6]$_4$ was obtained as a red solid: mp >250 °C; FABMS 2027 (M − PF_6)$^+$; ^{1}H NMR (CD_3COCD_3, 213 K) δ 3.29−3.34 (4H, m), 3.40−3.83 (42H, m), 3.87−4.03 (18H, m), 4.11−4.14 (4H, m), 5.97 (8H, s), 6.25 (4H, d, J_{AB} = 8 Hz), 6.36 (4H, d, J_{AB} = 8 Hz), 6.91 (4H, s), 7.97 (8H, s), 8.12 (8H, d, J = 7 Hz), 9.15 (8H, d, J = 7 Hz); ^{13}C NMR (CD_3COCD_3) δ 65.7, 68.3, 68.7, 70.5, 71.2, 116.3, 117.6, 126.5, 131.8, 137.7, 145.7, 147.1, 160.8 (not all the carbon atoms are observed, on account of the intermediacy of the rate of equilibration in the system at room temperature on the ^{13}C NMR time scale).

{[3]-[BBIPYBIXYCY]-[TPP68C20]-[BBIPYBIXYCY]catenane}-[PF_6]$_8$. A solution of [BBIPYXY][PF_6]$_2$ (390 mg, 0.55 mmol), TPP68C20 (100 mg, 0.09 mmol), and 1,4-bis(bromomethyl)benzene (180 mg, 0.68 mmol) in DMF (10 mL) was subjected to ultrahigh pressure (10 kbar) for 20 h. The reaction mixture was then quenched into a saturated aqueous solution of NH_4PF_6. Warming the solution to 50 °C completed the precipitation of the products. The dark red solid was filtered and then washed with H_2O, MeOH, and $CHCl_3$, and finally with Et_2O, before being dissolved in $MeNO_2$. Precipitation of polymeric impurities by the careful addition of $CHCl_3$ and subsequent filtration produced the crude product as a mixture of [2]- and [3]catenanes in $MeNO_2$. Fractional crystallization of the desired [3]catenane was obtained by the careful addition of $CHCl_3$ and the gradual cooling of the flask to −18 °C. The desired [3]catenane was isolated by filtration, washing the dark red crystals with $MeNO_2$ and Et_2O, and finally drying under high vacuum to afford {[3]-[BBIPYBIXYCY]-[TPP68C20]-[BBIPYBIXYCY]catenane}[PF_6]$_8$ as a dark red oil (34 mg, 11%): FABMS 3127 (M − PF_6)$^+$; ^{1}H NMR (CD_3CN) δ 3.55−3.89 (68H, br m), 5.66 (16H, s), 5.90−6.70 (8H, v br m), 7.67−7.71 (16H, m) 7.75 (16H, s), 8.83−8.87 (16H, m); ^{13}C NMR (CD_3CN, 343 K) δ 66.2, 68.8, 70.9, 71.7, 71.7, 115.6, 127.1, 132.1, 137.8, 145.9, 147.7, 152.8.

{[2]-[BPP34C10]-[BBIPYBIXYCY]catenane}[PF_6]$_4$. Method A. 1,4-Bis(bromomethyl)benzene (210 mg, 0.80 mmol), BPP34C10 (217 mg, 0.41 mmol), and 4,4′-bipyridine (125 mg, 0.80 mmol) were dissolved in dry DMF 915 mL). After stirring at room temperature for 5 days, a deep red precipitate appeared. This precipitate was filtered off, washed with $CHCl_3$, and dried. The resulting solid was redissolved in H_2O and treated with a saturated aqueous solution of NH_4PF_6. The resulting precipitate was collected, dried, and redissolved in the minimum volume (10 mL) of $MeNO_2$. Careful addition of $CHCl_3$ with cooling to −15 °C resulted in the precipitation of polymeric impurities. The solution was filtered while still cold and the solvent removed in vacuo to afford the crude [2]catenane. Recrystallization from MeCN/H_2O yielded a red solid which was characterized as {[2]-[BPP34C10]-[BBIPYBIXYCY]catenane}[PF_6]$_4$ (118 mg, 18%): mp >275 °C; FABMS [M − PF_6]$^+$, 1491 (M − PF_6)$^+$; ^{1}H NMR (CD_3CN) 3.32−3.39 (4H, m), 3.43−3.48 (4H, br s), 3.52−3.57 (4H, m), 3.59−3.65 (4H, m), 3.70−3.77 (4H, m), 3.81−3.86 (4H, m), 3.86−3.92 (8H, m), 3.93−3.97 (4H, m), 5.67 (8H, m), 6.16 (4H, s), 7.66 (8H, d, J = 7 Hz), 7.79 (8H, s), 8.85 (8H, d, J = 7 Hz); ^{13}C NMR (CD_3CN) 65.5, 67.3, 68.4, 70.0, 70.5, 70.8, 70.9, 71.4, 71.5, 113.8, 115.8, 126.4, 131.7, 137.7, 145.6, 146.9, 151.1, 153.0. Anal. ($C_{64}H_{72}N_4O_{10}P_4F_{24}$) C, H, N.

Method B. 1,4-Bis(bromomethyl)benzene (73 mg, 0.28 mmol), BPP34C10 (77 mg, 0.14 mmol), and 4,4′-bipyridine (44 mg, 0.28 mmol) were dissolved in dry DMF (*ca.* 8 mL). This solution was transferred to a Teflon high-pressure reaction vessel and sealed therein. The reaction mixture was subjected to a pressure of 12 kbar at 15 °C for 24 h. After this time, the reaction time was poured into H_2O (80 mL) and initial counterion exchange effected as described in method A. The resulting red solid was subjected to column chromatography [SiO_2, MeOH−2 N NH_4Cl−$MeNO_2$ (7:2:1)], and the catenane-containing fractions were combined. Counterion exchange as described previously yielded the pure {[2]-[BPP34C10]-[BBIPYBIXYCY]catenane}[PF_6]$_4$ (187 mg, 42%). This compound afforded spectroscopic data identical to those of the compound obtained using method A.

Method C. 4,4′-Bipyridine (0.78 g, 5.00 mmol) in MeCN (20 mL) was added to a refluxing solution of 1,4-bis(bromomethyl)benzene (8.00 g, 30.00 mmol) in MeCN (100 mL) over a period of 6 h. Heating under reflux was continued for 20 h with protection from moisture. The resulting precipitate was collected, washed well with chloroform, and dried. The counterions were exchanged for hexafluorophosphate ions as described previously. This crude dibromide (100 mg, 0.13 mmol) (single component on TLC) was then reacted with 4,4′-bipyridine (20 mg, 0.13 mmol) and BPP34C10 (66 mg, 0.13 mmol) in dry DMF for 4 days at room temperature. The resulting red-colored solution and precipitate were treated as described in method B to yield the pure {[2]-[BPP34C10]-[BBIPYBIXYCY]catenane}[PF_6]$_4$ (105 mg, 53%). This compound afforded spectroscopic data identical to those of the compound obtained using method A.

Electrochemistry. The electrochemical experiments were performed with a small volume (<1 mL), single-compartment cell obtained from Cypress Systems (Lawrence, KS). A disk glassy carbon electrode (0.0079 cm^2) and a platinum wire were used as working and auxiliary electrodes, respectively. All potentials were measured against an Ag/AgCl reference electrode. Tetrabutylammonium hexafluorophosphate (Fluka puriss) was used as the supporting electrolyte. HPLC-quality acetonitrile was refluxed over CaH_2 under a dry nitrogen atmosphere prior to distillation and use. Activated neutral alumina was also added to the test solution in the electrochemical cell for in situ drying of the solvent system. Cyclic voltammetry experiments were performed as already reported.[1] Half-wave potentials ($E_{1/2}$) were determined as the average of the corresponding anodic and cathodic peak potentials. Differential pulse voltammetry (DPV) was utilized in some cases to improve the resolution of overlapping voltammetric waves. From DPV data, half-wave potentials were determined by the simple equation $E_{1/2} = E_{peak} + \Delta E_p/2$, where E_{peak} is the peak potential value observed in the DPV response and ΔE_p is the pulse amplitude used in the excitation wave form. Typically, a pulse amplitude of 10 mV, a pulse width of 50 ms, and a scan rate of 4 mV/s were used for the generation of the excitation wave form.

X-ray Crystallography. For compounds and complexes A, D, and B (Table 8), respectively, X-ray diffraction measurements were performed on a Nicolet R3m diffractometer with graphite-monochromated Cu Kα radiation with ω scans. For compound C, data were measured on a Siemens P4/PC diffractometer with graphite-monochromated Mo Kα radiation using ω scans. Crystal data and data collection parameters are presented in Table 8. Lattice parameters were deter-

Table 8. Crystal Data and Data Collection Parameters

data	A[a]	B[a]	C[a]	D[a]
formula	$C_{30}H_{44}O_{11}$	$C_{42}H_{58}O_{11}N_2P_2F_{12}$	$C_{66}H_{76}N_4O_{11}P_4F_{24}$	$C_{104}H_{120}O_{20}N_4P_4F_{24}$
solvent		$1.2H_2O$	5MeCN	X[c]
molecular weight	580.7	1078.5	1886.5	2454.1
lattice type	orthorhombic	monoclinic	monoclinic	triclinic
space group	orthorhombic	monoclinic	monoclinic	triclinic
space group	$P2_1ab$	$P2_1/a$	$P2_1/c$	$P\bar{1}$
T (K)	293	293	293	293
cell dimensions				
a (Å)	8.123(2)	18.378(12)	13.881(12)	13.462(3)
b (Å)	15.854(3)	11.541(5)	23.106(9)	15.002(4)
c (Å)	23.502(4)	23.601(16)	27.187(10)	16.180(4)
α (deg)				72.40(2)
β (deg)		90.42(5)	92.62(2)	83.46(2)
γ (deg)				73.67(2)
V (Å^3)	3027	5006	8711	2988
Z	4	4	4	1
D_c (g cm^{-3})	1.27	1.43	1.44	1.36
$F(000)$	1248	2248	3896	1272
μ (mm^{-1})	0.76	1.73	0.20	1.51
θ range (deg)	2–58	2–58	4–22.5[b]	2–50
no. of unique reflections				
measured	2229	6558	11375	6127
observed	1849	4034	5971	3126
no. of variables	371	672	1115	710
R (%)	4.8	11.34	10.7	13.0
R_w (%)	5.1	11.74	10.3	14.3
weighting factor f	0.000 96	0.0008	0.0008	0.004 50
extinction g	0.0009(3)	0.000 06(10)		0.0018(7)

[a] A = [BPP37C11]; B = [BPP37C11·PQT·2H$_2$O[PF$_6$]$_2$; C = {[2]-[BPP37C11]-[BBIPYBIXYCY]catenane}[PF$_6$]$_4$; D = {[3]-[BPP34C10]-[BBIPYBIBTCY]-[BPP34C10]catenane}[PF$_6$]$_4$. [b] Mo Kα radiation. [c] X corresponds to unidentified partial occupancy solvent fragments.

mined by least-squares fits from 18 to 22 centered reflections. Intensities were corrected for the decay of two control reflections, measured every 50 reflections, and for Lorentz and polarization factors but not for absorption.

The structures were solved by direct methods and refined by full-matrix least squares. Reflections with $|F_o| > 3\sigma(|F_o|)$ were considered to be observed and were included in the refinements (based on F_o). A weighting function of the form $w^{-1} = \sigma^2(F) + pF^2$ was applied. Leading hydrogen atoms on methyl groups attached to sp^2 carbon atoms were, where possible, located from the ΔF maps. Methyl groups were refined as idealized rigid bodies. In compound C, the hydrogen atoms of the included MeCN molecules could not be located; they were therefore omitted from the computations. In compound D, the included solvent was fragmented and could not be identified. The residual electron density was reduced by refining partial weight C and O atoms in this region of the structure. Depending on data quality and the data: parameter ratio, hydrogen atoms were either included in the refinement or placed in calculated positions (C–H distance 0.96 Å) and allowed to ride on their parent carbon atoms (U(H) = 1.2U_{eq}(C)).

Parameters refined were the overall scale factor, isotropic extinction parameter g (correction of F_c where $F^* = F_c[1.0 + 0.002gF^2/\sin(2\theta)]^{0.25}$), and positional and anisotropic thermal parameters for the full occupancy non-hydrogen atoms. Refinements converged with shift: error ratios less than unity for all variables, except occasionally for disordered atoms. Final difference Fourier maps showed no significant features. All calculations were carried out using the SHELXTL program system.[46]

(46) Sheldrick, G. M. *SHELXTL PLUS PC*, Version 4.2; Siemens Analytical X-ray Instruments Inc.: Madison, WI, 1990.

Acknowledgment. This research was supported by the Science and Engineering Research Council in the United Kingdom, and a NATO Grant (SRG 920666) from Supramolecular Chemistry Program for the work carried out in Miami. We gratefully acknowledge the assistance of Kratos Analytical (Manchester, U.K.), and in particular Dr. M. Kimber, Dr. H. Wight, and Dr. J. Moncur, in the collection of the LSI mass spectra reported in this paper. We thank Fisons Instruments Organic Analysis Limited (Wythenshawe, U.K.), and in particular D. J. Pugh, for assistance in the collection of the ES mass spectrum reported here.

Supplementary Material Available: Tables giving the structure determination summary, atomic coordinates, temperature factors, bond lengths and angles, and torsion angles for [bis(*p*-phenylene)-37-crown-11·paraquat][PF$_6$]$_2$ and {[2]-[bis(*p*-phenylene)-37-crown-11]-[cyclobis(paraquat-*p*-phenylene)]-catenane}[PF$_6$]$_4$ (27 pages). This material is contained in many libraries on microfiche, immediately follows this article in the microfilm version of the journal, and can be ordered from the ACS; see any current masthead page for ordering information.

JA942848R